NEWTON-RAPHSON BASED LOAD FLOW ANALYSIS OF AC/DC DISTRIBUTION SYSTEMS WITH DISTRIBUTED GENERATION

A THESIS SUBMITTED TO
THE GRADUATE SCHOOL OF NATURAL AND APPLIED SCIENCES
OF
MIDDLE EAST TECHNICAL UNIVERSITY

BY

FERHAT EMRE KAYA

IN PARTIAL FULFILLMENT OF THE REQUIREMENTS
FOR
THE DEGREE OF MASTER OF SCIENCE
IN
ELECTRICAL AND ELECTRONICS ENGINEERING

SEPTEMBER 2019

Approval of the thesis:

NEWTON-RAPHSON BASED LOAD FLOW ANALYSIS OF AC/DC DISTRIBUTION SYSTEMS WITH DISTRIBUTED GENERATION

submitted by **FERHAT EMRE KAYA** in partial fulfillment of the requirements for the degree of **Master of Science in Electrical and Electronics Engineering Department, Middle East Technical University** by,

Prof. Dr. Halil Kalıpçılar
Dean, Graduate School of **Natural and Applied Sciences** _____

Prof. Dr. İlkay Ulusoy
Head of Department, **Electrical and Electronics Engineering** _____

Prof. Dr. Ali Nezih Güven
Supervisor, **Electrical and Electronics Engineering, METU** _____

Examining Committee Members:

Prof. Dr. Işık Çadırcı
Electrical and Electronics Engineering, Hacettepe University _____

Prof. Dr. Ali Nezih Güven
Electrical and Electronics Engineering, METU _____

Assoc. Prof. Dr. Murat Göl
Electrical and Electronics Engineering, METU _____

Assist. Prof. Dr. Ozan Keysan
Electrical and Electronics Engineering, METU _____

Assist. Prof. Dr. Emine Bostancı
Electrical and Electronics Engineering, METU _____

Date: 05.09.2019

I hereby declare that all information in this document has been obtained and presented in accordance with academic rules and ethical conduct. I also declare that, as required by these rules and conduct, I have fully cited and referenced all material and results that are not original to this work.

Name, Surname : Ferhat Emre Kaya

Signature :

ABSTRACT

NEWTON-RAPHSON BASED LOAD FLOW ANALYSIS OF AC/DC DISTRIBUTION SYSTEMS WITH DISTRIBUTED GENERATION

Kaya, Ferhat Emre
MS, Department of Electrical and Electronics Engineering
Supervisor: Prof. Dr. Ali Nezih Güven

September 2019, 94 pages

Increasing concerns about climate change and global pollution rates emphasized the importance of renewable energy resources. Rising pressure to utilize green energy alternatives requires some changes and rearrangements on the available alternative current (AC) oriented electric power system. Moreover, electric charging stations, renewable and distributed electricity sources like battery storage systems, solar power plants use direct current (DC) and additional power conversion is needed for their integration into the current distribution network. This explains why hybrid AC/DC smart grid concepts are developed.

Although there are various load flow analysis approaches applied on hybrid AC/DC transmission systems, not much work is proposed at the distribution system level. The scope of the thesis is to develop an integrated load flow approach for AC/DC distribution networks, which include a variety of power electronic devices as well as distributed energy sources. In the method presented, AC and DC power flow equations are combined and solved using Newton-Raphson algorithm with a modified Jacobian matrix. Commonly used DC/DC converters and voltage source

converters present in the grid are represented with their respective models. This load flow calculation method is implemented on MATLAB and simulations are performed for different distribution test systems, which utilize a variety of converter models and load profiles. Solution of the proposed load flow algorithm has shown consistency with the results obtained by other approaches.

Keywords: Load Flow Analysis, Hybrid AC/DC Distribution System, Voltage Source Converter, Smart Grid, DC/DC Converter

ÖZ

DAĞITIK ÜRETİMLİ AA/DA DAĞITIM SİSTEMLERİNİN NEWTON-RAPHSON TABANLI YÜK AKIŞI ANALİZİ

Kaya, Ferhat Emre
Yüksek Lisans, Elektrik ve Elektronik Mühendisliği Bölümü
Tez Yöneticisi: Prof. Dr. Ali Nezih Güven

Eylül 2019, 94 sayfa

İklim değişikliği ile küresel kirlilik seviyeleri hakkındaki artan endişeler yenilenebilir enerji kaynaklarının önemini vurgulamaktadır. Çevreci enerji alternatiflerinin kullanılması konusundaki artan baskı mevcuttaki alternatif akım (AA) odaklı elektrik güç dağıtım sistemlerinde bazı değişiklikleri ve yeniden düzenlemeleri gerektirmektedir. Ayrıca, elektrik şarj istasyonları ile batarya depolama sistemleri, güneş santralleri gibi yenilenebilir ve dağıtık elektrik kaynakları doğru akım (DA) kullanmakta ve bunların mevcut dağıtım şebekesine uyumlanması ek güç dönüşümleri gerektirmektedir. Bu da hibrit AA/DA akıllı şebeke kavramlarının neden geliştirildiğini açıklamaktadır.

Hibrit AA/DA iletim sistemlerinde birçok yük akışı yaklaşımları bulunurken, dağıtım sistemleri seviyesinde pek bir çalışma sunulmamıştır. Bu nedenle, bu tezin amacı, çeşitli güç elektroniği cihazlarını ve dağıtık enerji kaynaklarını bünyesinde barındıran hibrit AA/DA dağıtım şebekeleri için bütünleşik yük akış analizi yaklaşımı geliştirmektir. AA ve DA denklemleri bütünleşik olarak değiştirilmiş Jakobiyen matrisi ile Newton-Raphson yöntemi kullanılarak çözülmektedir.

Şebekede yaygın olarak kullanılan DA/DA çeviriciler ve gerilim kaynaklı dönüştürücüler ilgili modelleri ile birlikte sunulmuştur. Buradaki yük akışı hesaplama metodu MATLAB üzerinde uygulanmış, çeşitli dönüştürücü modelleri ve yük profilleri içeren farklı dağıtım test sistemleri için benzetimler gerçekleştirilmiştir. Önerilen yük akış algoritmasının çözümü diğer yaklaşımlar kullanılarak üretilen sonuçlar ile tutarlılık göstermiştir.

Anahtar Kelimeler: Yük Akışı Analizi, Hibrit AA/DA Dağıtım Şebekesi, Gerilim Kaynaklı Dönüştürücü, Akıllı Şebeke, DA/DA Dönüştürücü

To My Family and Friends

ACKNOWLEDGEMENTS

Firstly, I would like to thank my supervisor Prof. Dr. A. Nezih Güven for his technical and motivational support, encouragement and helpful advices through all stages of this master thesis.

I wish to express my appreciation to my colleague Dr. Emre Durna for his great guidance and suggestions for this research. I also thank my friends for giving me motivation and support through writing this thesis.

Finally, I would like to express my sincere gratitude to my family for providing me continuous support and endless love in my journey towards this degree. Last and foremost, I would like to thank Allah SWT, the Almighty for giving the knowledge, courage and strength to cope with difficulties in my life and chance to complete this thesis.

TABLE OF CONTENTS

LIST OF TABLES

TABLES

LIST OF FIGURES

FIGURES

LIST OF SYMBOLS

P_n^{spec}	Specified active power injected at bus n.
Q_n^{spec}	Specified reactive power injected at bus n.
P_n^{calc}	Calculated active power injected at bus n.
Q_n^{calc}	Calculated reactive power injected at bus n.
$P_n^{G,AC}$	Active power generated by the AC generator connected at bus n.
$P_n^{G,DC}$	Active power generated by the DC generator connected at bus n.
$P_n^{L,AC}$	Active power consumed by the AC load connected at bus n.
$P_n^{L,DC}$	Active power consumed by the DC load connected at bus n.
$Q_n^{G,AC}$	AC generator reactive power connected at bus n.
$Q_n^{L,AC}$	Reactive power consumed by the AC load connected at bus n.
$Q_n^{G,DC}$	Injected reactive power by the converter of DC generator connected at bus n.
$Q_n^{L,DC}$	Reactive power consumed by the converter of DC generator connected at bus n.
M_{nm}	Modulation index of the VSC between bus n and bus m.
D_{nm}	Duty ratio of the DC/DC converter between bus n and bus m.
N_{Bus}	Total number of buses.

N_{PV}	Total number of PV buses.
N_{PQ}	Total number of PQ buses.
N_{DCL}	Total number of DC Load buses.
N_{ACCV}	Total number of AC voltage controlled buses.
N_{DCCV}	Total number of DC voltage controlled buses.
Y_{nm}	(n,m)th entry of the bus admittance matrix.
G_{nm}	(n,m)th entry of the real part of the bus admittance matrix.
B_{nm}	(n,m)th entry of the imaginary part of the bus admittance matrix.
P_{nm}^{AC}	AC side active power flow from bus n to bus m.
Q_{nm}^{AC}	AC side reactive power flow from bus n to bus m.
P_{nm}^{DC}	DC side active power flow from bus n to bus m.
I_{nm}^{DC}	DC current flowing from bus n to bus m.
V_n	Magnitude of the voltage at bus n in p.u.
θ_n	Voltage angle of bus n in degrees or radians.
φ_{VSC}	Power factor angle of the voltage source converter.
g_{nm}	Line conductance between bus n and bus m.
b_{nm}	Line susceptance between bus n and bus m.
η	Converter efficiency in %.

CHAPTER 1

INTRODUCTION

1.1 Background and Contribution

World is trying to take urgent actions to reduce greenhouse emissions produced by the electricity sector since fossil fuels are mainly used to generate electricity. In order to have a more sustainable and environmentally friendly energy system, the electricity generation procedure is changing from fossil fuel dominant structure towards a more renewable and distributed one. Therefore, many countries are trying to adapt renewable energy resources to their electric power system while they are also working hard to meet their increasing electricity demand.

Until today, power systems were mostly one directional in a way that generated electricity was being transferred by transmission systems to distribution systems where consumers are connected. As of today, however, electricity can be generated and consumed within the distribution system resulting in a bidirectional power flow. Additionally, EV charging stations may behave as generators to supply surplus energy to the utility grid and battery systems may behave like loads when they are getting charged. Therefore, overall complexity of the system increases and the electrical power system evolves into a smart and AC/DC hybrid structure.

The fact that present distribution systems need to adapt increasing utilization of DC generators and loads implies that the traditional AC oriented power flow analysis also needs to change to meet new requirements for a hybrid power system. Many researches are presented on AC/DC load flow with focus on high voltage DC

(HVDC) transmission systems in the literature but these methods are not convenient for hybrid distribution systems since those methods are weak for systems where DC bus penetration is high and that increases complexity of the algorithm. Additionally, it is most probable that future smart AC/DC distribution systems will have several intersecting AC and DC nodes, branches, different AC or DC generators and loads coupled together, therefore decoupled methods which separate main AC/DC grid into several subgrids may not be suitable to be applied for coupled AC/DC distribution systems [1]. Moreover, it is stated in [2] that compared to the unified method, the sequential method is more complex, may have convergence problems in some cases and takes more time to converge to a solution because whole AC solution must be recalculated each time for a parameter update on the DC side. It is also indicated for the sequential method that algorithm reliability decreases and becomes more complex as the iterative loop number increases [3]. The advantage of Newton-Raphson iterative method is that it converges faster than other approaches owing to its quadratic feature. Therefore, this thesis have focused on an integrated methodology for load flow analysis of AC/DC distribution systems that are combinations of AC and DC microgrids.

The proposed approach contributes such that a Newton-Raphson based iterative method for overall system level power transfers between AC and DC sub-networks is presented by utilizing AC/DC voltage source converters and several possible connection types in a hybrid distribution system with DC/DC converters are considered. Proposed load flow method takes into account all converter losses and is able to obtain power flow through converters connected at different buses. This method helps to reduce algorithm complexity and has the advantage of faster convergence speed with high accuracy compared to other approaches by combining AC and DC line flows. The researchers of [1] proposed a unified load flow analysis approach based on reduced gradient method for AC/DC distribution systems. However, that method lacks DC/DC converter models and operating modes of the converters such as constant voltage control and constant duty ratio are ignored. Future smart AC/DC grids are expected to include various AC/DC and DC/DC converters, therefore converter parameters and their losses should be calculated in

the load flow analysis as well. In the proposed method, commonly used DC/DC converter models, which are required to control DC bus voltages, are implemented and different operating modes are considered for those converters. Power flow equations and derivatives with respect to system unknowns are obtained for different system configurations. The method in [1] has used only constant modulation index mode of the AC/DC VSC; however, the method presented in this thesis also utilizes constant output voltage mode of the voltage source converter and determines the required modulation index for providing specific voltage magnitude at the converter output bus. Additionally, DC/DC converters are utilized in constant duty ratio and constant output voltage modes and since presented equations are generic, other converter models can be implemented on the proposed method.

1.2 Thesis Outline

Firstly, a brief information about distribution system topologies is provided at the beginning of the second chapter. Hybrid AC/DC distribution systems are explained and integration of distributed generators to those systems is investigated. At the last section of the second chapter, previous studies on hybrid AC/DC smart grids are briefly mentioned. In the third chapter, voltage source converter that is utilized for AC to DC conversion and commonly used DC/DC converter models are provided. Afterwards, derivation of power flow equations and Newton-Raphson iteration are explained. Then, the implementation of this iterative solution procedure in an AC system and AC/DC hybrid system is described and line power flow equations are given for different connection topologies.

Proposed algorithm is implemented on a variety of test systems and results are given in the fourth chapter. Moreover, the results produced by the presented method and other approaches are compared in this chapter. Finally, outcomes of the proposed load flow calculation method are evaluated in the last chapter.

CHAPTER 2

AN OVERVIEW OF THE DISTRIBUTION SYSTEM

2.1 AC vs DC

Although electric power systems are mainly dominated by alternating current today, the end of 19th century was a battleground for alternating current (AC) and direct current (DC) systems. Towards the end of 1880s, times when Edison was standing on the side of DC electricity, the inability to control DC voltage level was an obstacle in front of widely spreading of DC systems. Power electronics were not developed back then to have the ability to regulate the DC voltage to higher or lower levels. This has brought the problem that DC machines were limited to generate low voltages for safety issues and this has caused serious losses during the transmission of electricity, meaning that electricity transmission was restricted to a few hundred meters.

On the other hand, the AC side, at which Tesla was proposing, had a significant advantage with the transformer that gives opportunity to adjust voltage in different levels. Because transformers made it possible to increase the AC voltage levels to kilovolts (kVs), losses on transmission lines are lower, therefore electricity can be transmitted over longer distances. When it has reached to destination, voltage can be reduced back to levels that will be utilized with the help of transformers again. At the end of this rivalry, AC side has dominated the electric power system leaving DC behind. AC transmission and distribution have established superiority and thus, AC generation machines and AC loads constituted a large part of the electric power system [4].

2.2 An Overview of AC Distribution Systems

At the beginning, transmission lines were bound to only a few kilometers and voltage and power levels were not very high for the first installed three-phase ac systems, but it has extended all over the world afterwards. Thanks to AC transformers, voltage is increased to higher levels to reduce losses during the transmission of electricity and it is decreased back to levels that match the consumer demand. Considering that generation of electricity, load side and transmission systems are mainly relied on AC until today, it becomes evident that AC electric power system has gained a valuable place in the 20th century.

In general, a distribution system serves in-between transmission system and customers. Typical AC distribution systems can be investigated in two categories as primary distribution systems and secondary distribution systems. Primary distribution systems are composed of 3 wire, 3 phase and they are designed for greater voltage levels than normal utilization level for the specific needs of customers in the system as illustrated in Figure 1, whereas secondary distribution systems as shown in Figure 2, are composed of 4 wire, 3 phase and they are connected to typical customers. While 230 V is mainly used in secondary distribution systems, 33 kV, 11 kV and 6.6 kV are common levels in the world for primary distribution systems [5].

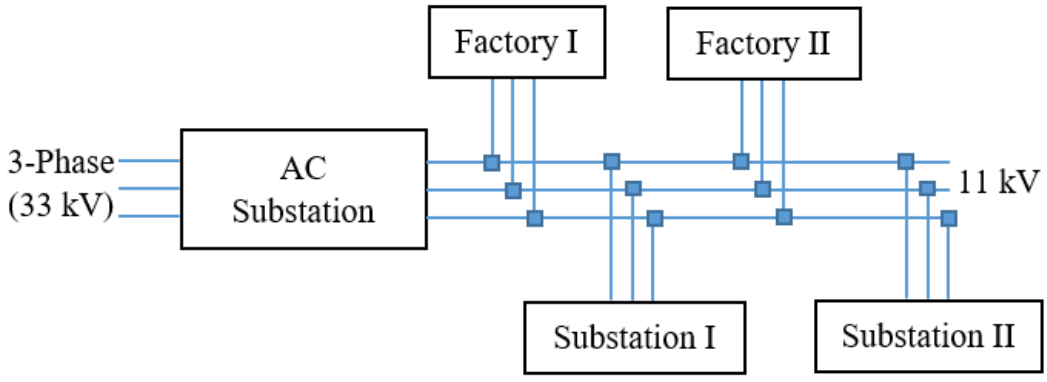

Figure 1. A Representative Schema for a Primary Distribution System

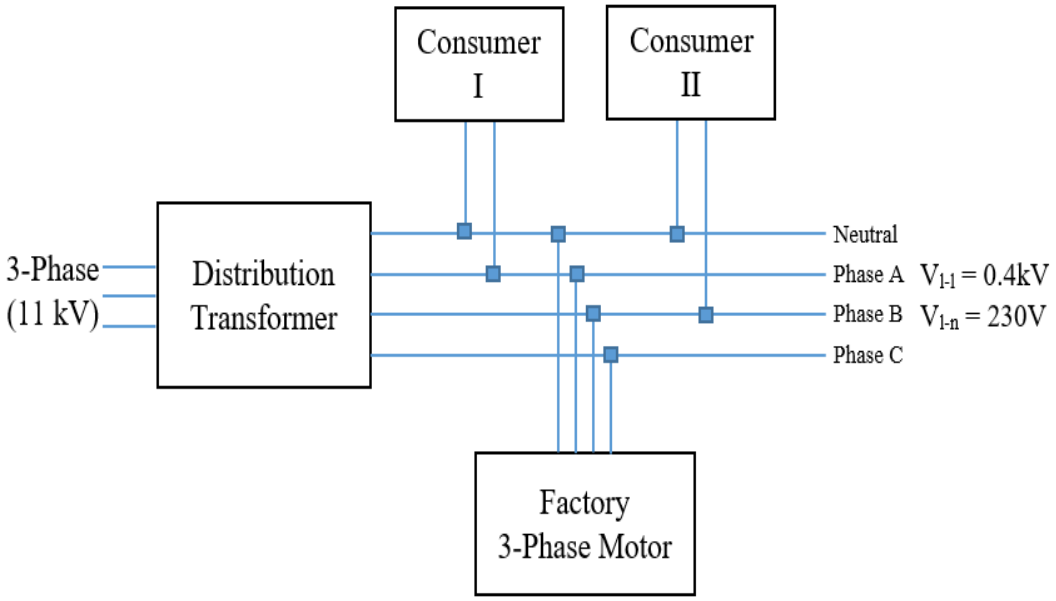

Figure 2. A Representative Schema for a Secondary Distribution System

Widespread utilization of distributed renewable generators changes the traditional grid structure and this tendency increases at a fast pace. International Renewable Energy Agency (IRENA) predicts that renewable portion of the total generation is going to reach 59% in 2030 [6].

Besides, SolarPower Europe's findings indicate that solar generation is growing faster than any other electricity generation source as shown in Figure 3 [7]. In 2017, newly installed solar power capacity was greater than any other power source and more than the total added capacity of fossil fuels and nuclear.

This report also suggests three different global market scenarios and it predicts that global solar power plant generation capacity could hit 1,270.5 GW in 2022 for the best-case scenario as illustrated in Figure 4.

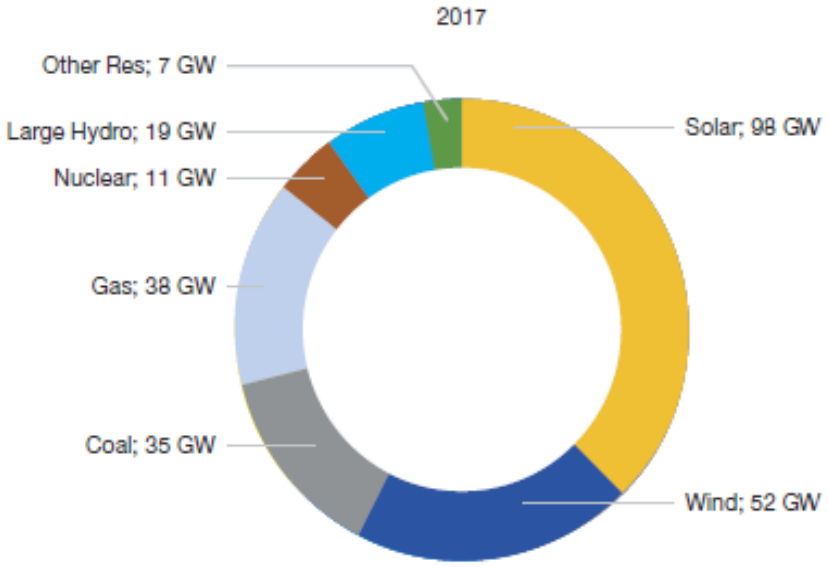

Figure 3. Net Power Generating Capacity Installed in 2017 in the World [7]

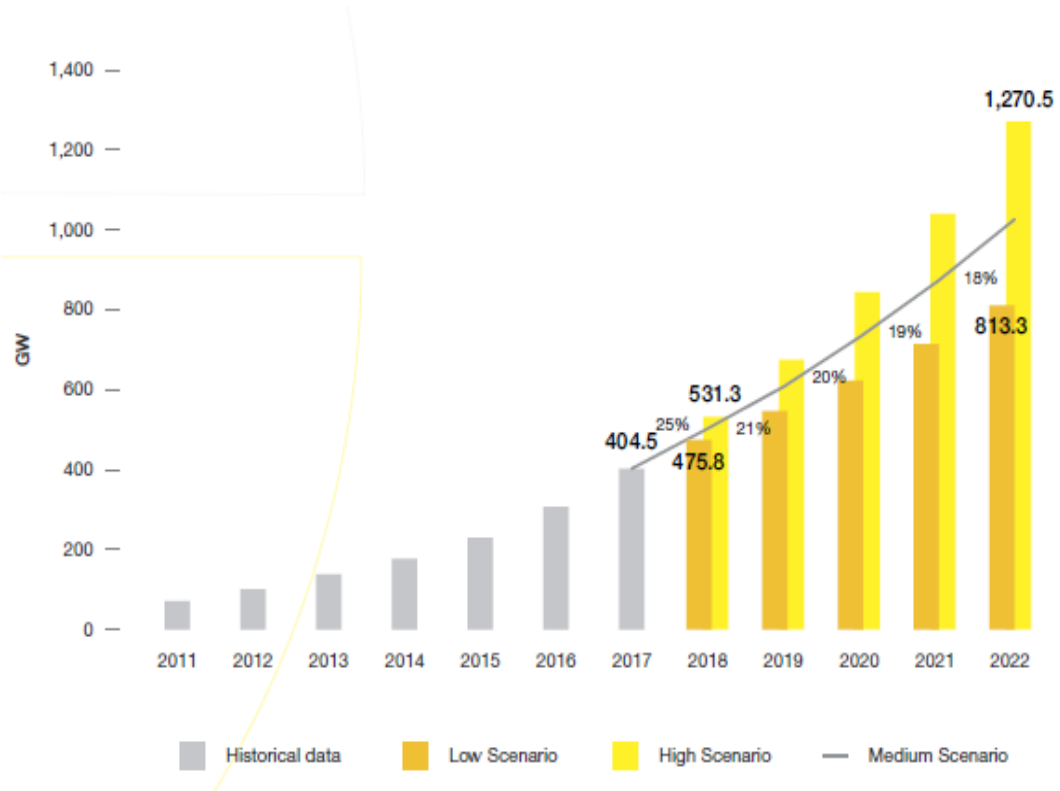

Figure 4. World Total Solar Market Scenarios between 2018 and 2022 [7]

In addition to solar power plants, other distributed generators (DGs) like battery storage systems and fuel cells are all connected to the distribution grid and a significant portion of these sources have DC outputs. For this reason, DC output of these generators should be converted to AC before connecting to the distribution network. Even wind turbines require power converters to synchronize output voltage with the AC distribution system voltage level and frequency.

Not only did generation side change, the load side of the electrical power system has also changed since most devices in our lives require low voltage DC supply. In the present distribution system computers, televisions, mobile phones, household appliances, led lightings are all connected to the AC distribution system by a bunch of converters. Figure 5 illustrates a representative schema for an AC grid.

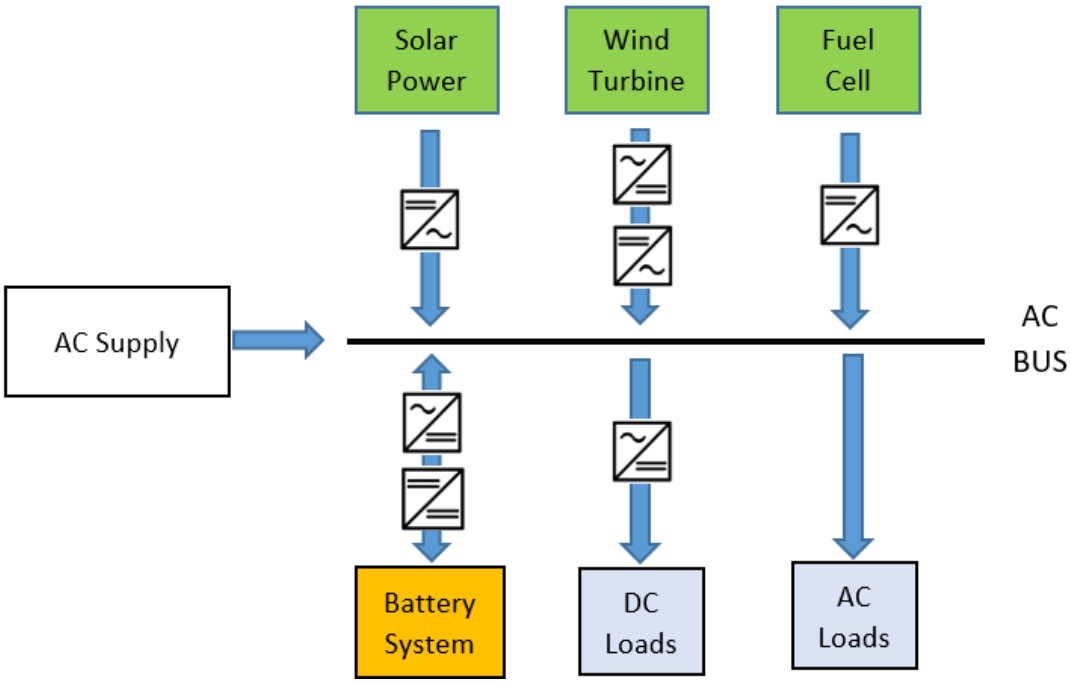

Figure 5. Representation of an AC Grid with DGs, Battery and Loads

2.3 DC Distribution Systems

Although it is still valid that today's electric power system is mainly dominated by AC, increasing utilization of wind turbines and solar power plants, new type of DC loads like electric vehicles (EVs) and DC motor drives, and also battery storage systems are challenging the structure of current distribution systems. This tendency indicates that DC systems are going to be more important for the future electric power systems. For this reason, new technologies utilizing efficient and convenient use of DC systems have gained popularity again with the support given by advances in power electronics field [8].

In order to implement DC sources such as solar power plants or battery storage systems to the AC distribution grid, DC to AC conversion is necessary which results in a power loss during the process. Besides, since a significant portion of home appliances like televisions, computers and EV charging stations require DC, there is a rising trend of providing DC power directly to these devices [9]. However, under the current situation, devices which rely on DC are connected to an AC distribution system at homes or offices, therefore another process is needed. This conversion process cuts about 4-15% percent of the input power and the total loss increases when more converters are implemented in the system [10]. Hence, rather than such multi-level conversion processes, AC electrical systems may be extended with DC distribution systems removing some power electronic circuits.

For the load side, it should be noted that many loads today incorporate power electronic devices for AC to DC power conversion. This results in harmonic current injection to the utility and therefore lowering the power quality of the system. Hence, loads are accompanied by a variety of circuits for power factor correction in order to eliminate those undesirable effects. If a suitable DC voltage level is chosen, loads could have a straight connection to the network without AC/DC conversion and power factor correction circuitries [11].

It is presented in Table 1 that when a fuel cell, which produces DC power, connected to a residential DC distribution network, better results could be obtained in terms of total efficiency [12].

Table 1. Efficiency Comparison of a Residential Fuel Cell System [12]

	Connected to a DC System		Connected to an AC System	
Device	Conversion Stages	Efficiency (%)	Conversion Stages	Efficiency (%)
Kitchen Appliances	1	97.6	2	95.2
Home Electronics	2	95.2	5	88.4
Lights-Fluor.	2	95.2	4	90.6
Heating, Ventilation	1	97.6	2	95.2
Laundry Appl.	1	97.6	2	95.2
Weighted Ave.		**97.3**		**94.5**

Moreover, if a DC source has a direct connection to a DC distribution network, it could provide cost advantage, reduced complexity and increased efficiency when compared to the case where it supplies energy through some power electronic devices to an AC system [13].

In general, DC distribution systems are classified in two configurations as unipolar and bipolar distribution systems [14]. Unipolar DC distribution systems consist of one positive and one negative lines as shown in Figure 6, while bipolar DC distribution systems have three lines, one for positive, one for negative and one for neutral as illustrated in Figure 7. Loads may be connected to the positive voltage (+V), negative voltage (-V) or between them to double the voltage magnitude (2V) in a bipolar configuration.

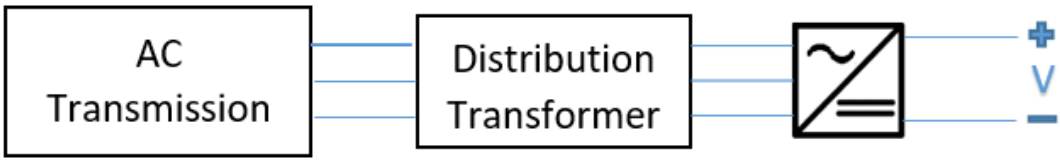

Figure 6. Unipolar DC Distribution System

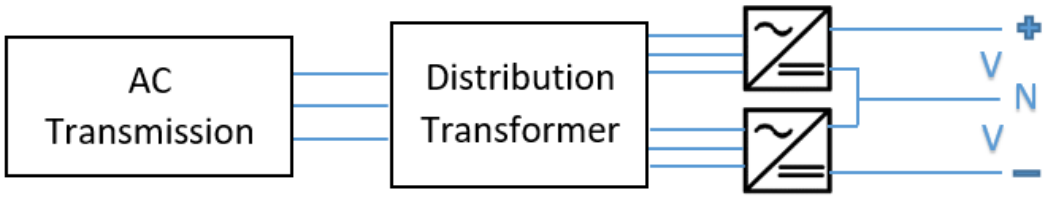

Figure 7. Bipolar DC Distribution System

A bipolar configuration can be beneficial such that if there is a fault in one of the positive or negative poles, the other pole can continue to supply power to the system. In both of these systems, a variety of converter types for DC/DC conversion or inverters for DC/AC conversion can be implemented according to different load types. A representative DC grid is shown in Figure 8.

In this representative DC grid model, EV charging station is allowed to conduct bidirectional power flow. Since some EV charging stations have solar panels on top, they can supply power to the grid when they are not fully occupied [15]. Battery storage systems also require bidirectional power flow since they are charged during excessive amount of power available and discharged during peak hours of electricity consumption occurs.

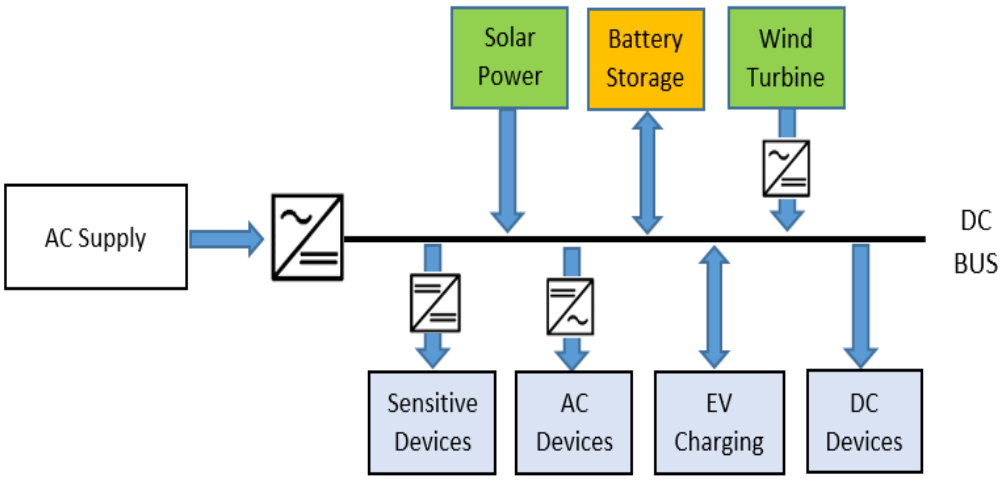

Figure 8. A Typical DC Grid with DGs, Battery and Loads

It is already stated that DC distribution systems are convenient to be supplied by solar power systems, battery storages or fuel cells whose outputs are DC. In addition to them, a DC distribution system can be also convenient for variable speed wind turbines, and microturbines. Although these systems produce AC power, because there is a requirement to synchronize output frequency of these generators before connecting to the AC distribution system, they include converters that first transform AC to DC power and afterwards DC to AC again. However, if they are connected directly to DC distribution networks, simpler converters can replace the formerly mentioned ones [11].

Other than these, DC distribution systems provide some advantages compared to their AC counterparts. According to Low Voltage Directive [16], DC systems are allowed to conduct higher voltages resulting in higher rms voltage value and increased power transfer capability. Hence, cable cross-sections and losses can be reduced with the help of higher power transfer capability. Fluctuations and temporary drops on voltage waveforms can be reduced at the consumer end with the implementation of power electronic converters and filters. When all these are put together, economically advantageous systems can be designed regarding capital and

operational costs [17]. However, when more power electronic circuitries are implemented in the system, probability of encountering problems increases. Although converters and filters increase the power quality at the consumer end, these devices inject some undesirable harmonics to the system and they have shorter lifetimes compared to other usual system components [18].

Because there are some differences on safety considerations between DC systems and AC systems, moving towards DC grid should be carefully studied in terms of following topics [19]:

- Circuit protection
- System maintenance
- Fault detection

In addition to protection, maintenance schemes and fault detection mechanisms, standardization of system components and voltage levels are other topics on the agenda for DC distribution systems.

2.4 Hybrid AC/DC Distribution Systems

After having mentioned about pure AC and DC distribution systems, it would be appropriate to mention another alternative involving both, namely a hybrid one. Although the electrical system is adapting towards a more sustainable and green future, the integration of renewables and energy storage systems require new updates and innovative solutions on the distribution network.

International Renewable Energy Agency suggests that renewable sources will be responsible for more than 80% of global electricity generation by 2050 and 52% of total electricity produced will be contributed by just wind and solar power plants [6]. As illustrated in Figure 9, the reference scenario indicates that total installed capacity can achieve more than 8000 GW in 2030 and over 12000 GW in 2050 with majority

of increase contributed by solar and wind power. For an alternative doubling scenario solar and wind capacity increase more than the reference scenario. As Figure 10 shows, remap scenario predicts generation using oil becomes zero and renewable electricity generation will be responsible for 82% of the total generation in 2050 [6]. These predictions indicate that the electrical system is going to become more decentralized with the increasing share of distributed generations.

Generation side and load side should be in equilibrium for an electrical system to achieve a flawless, secure and predictable operations. One drawback of renewable power generation sources is uncertainty associated with them. Their generation highly depends on instantaneous weather conditions.

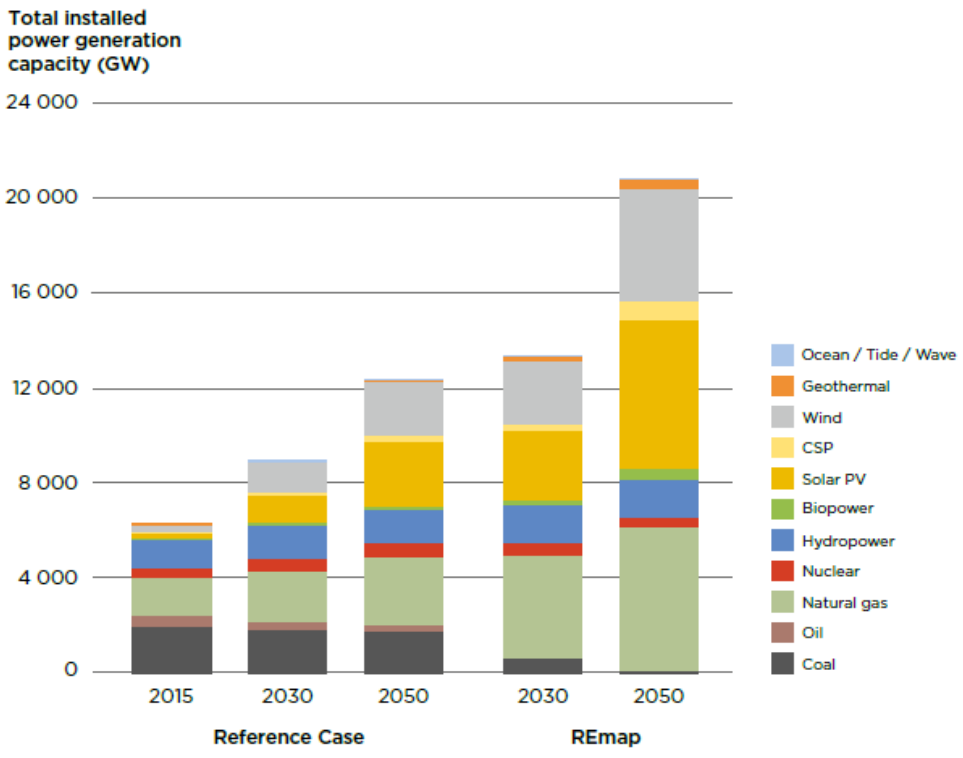

Figure 9. Power Generation Capacity for the Reference and Remap Cases between 2015 and 2050 [6]

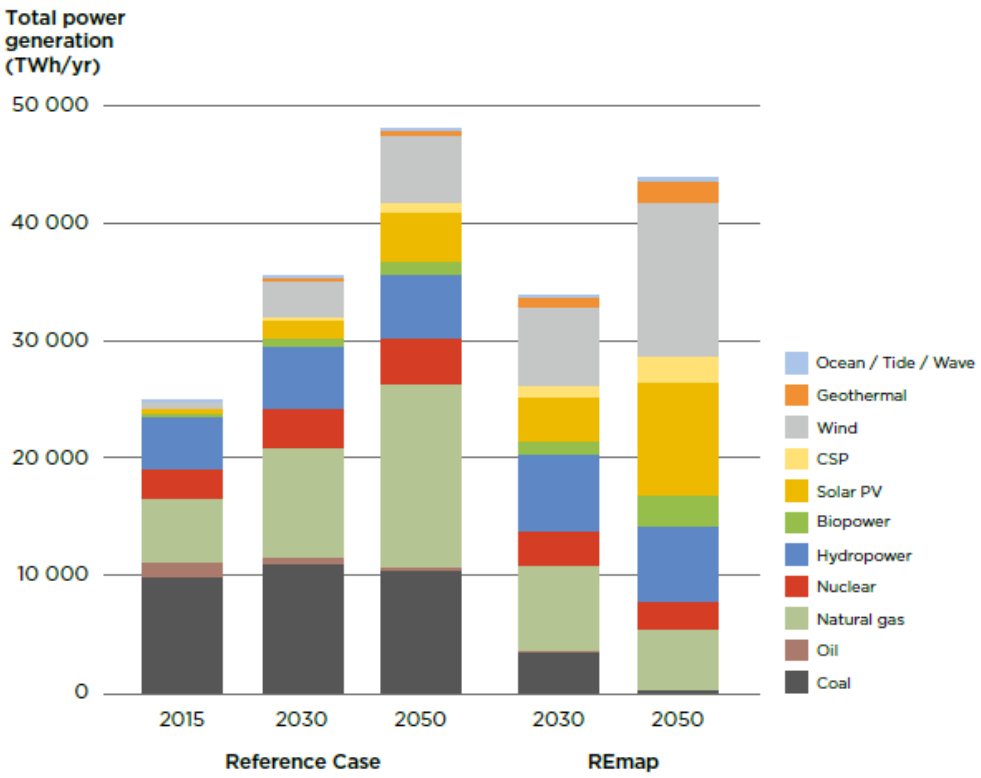

Figure 10. Power Generation for Two Cases between 2015 and 2050 [6]

For solar power plants, although algorithms like maximum power point tracking (MPPT) are implemented to make solar panels operate at their maximum efficient point in order to produce maximum power, their electricity generation is affected greatly by the temperature of solar panels or the radiation during the day. The power generation of a solar power plant is higher on sunny days or it decreases when it is a cloudy day. For wind turbines, the output power is again determined by the rotor size, season of the year, wind speed and altitude.

Other than these uncertainties, there are also much fundamental reasons that such power plants cannot produce electricity all the time because for solar power plants, there is no sunlight during night or for wind farms, no wind blows sometimes and all blades stop turning. In some cases, some of the wind turbines are running but some are not in the same power plant because wind only blows in a certain area, therefore reducing the great portion of the output power. For this reason, they may not be fully utilized every time.

On the other hand, electricity demand is increasing on a great pace today and consumers demand uninterrupted supply for their applications. Offices, commercial buildings, hospitals and even some devices in homes require continuous electrical energy. Therefore, battery storage systems are utilized to guarantee uninterrupted electricity supply. International Renewable Energy Agency predicts that battery storage system costs would be more than 50% cheaper by 2030 [6]. That means battery storage system installation would be more common to support the grid for smoother operation of services.

As shown in Figure 11, International Renewable Energy Agency predicts low and high case scenarios. The biggest increase comes from rooftop photovoltaics (PVs) for both scenarios [6].

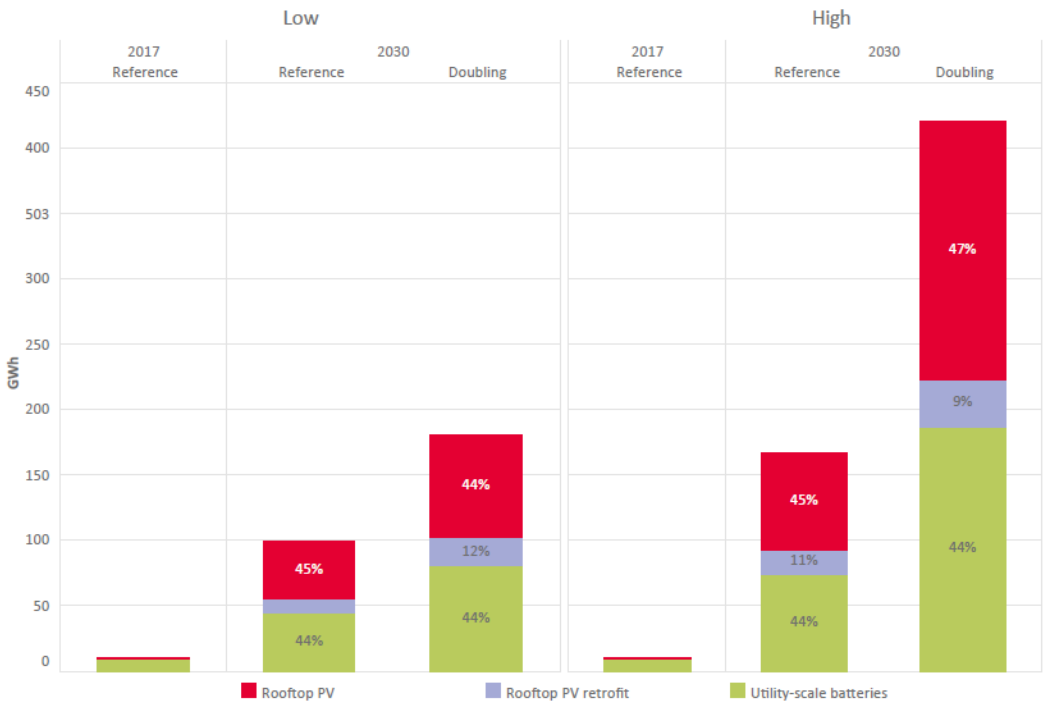

Figure 11. Global Capacity Increase for Battery Storage System in Stationary Applications by Sectors from 2017 to 2030 [6]

There is also a big growth for the utility-scale installation. These systems can be implemented for services like frequency control, reserved generation or market balancing. Therefore, present distribution network faces some challenges with the integration of distributed generators, modern electronic loads and penetration of EVs. Uncertainty present in all of these and further they may lead to problems like system overloading, voltage distortions and frequency fluctuations.

As covered in Section 2.3, DC distribution systems have some advantages especially when DC generating distributed sources are connected to the DC system. Even for some distributed AC generators like microturbines or wind turbines, DC system eases the connection of these generators by eliminating synchronization stages and it is more flexible since reactive power control is not required. By allowing the deployment of energy storage systems, DC network increases the overall system quality and makes the electrical system more immune to faults.

However, transition from an AC structure to a complete DC structure brings many problems with it. Distribution systems mainly rely on AC today and whole system established over many years with many investments. As an alternative, hybrid structures that are fundamentally AC but at the same time, incorporating DC network interconnections are proposed.

First of all, a DC grid sub-system may be employed in a present AC distribution system to enhance the capability of the network. Active power and reactive power may be transferred between AC buses and an interfacing converter to adjust the voltage on the AC terminal. Active power can be injected to the DC network when it is needed or DC grid can supply excessive energy to the AC side. The system gains additional power handling capability [20].

While the operational principle is different, AC and DC systems can be interconnected with the implementation of power electronic devices. Advancements in power electronics, automation and control technologies enable conventional distribution systems to get benefits of DC systems. Distributed generators penetration has also changed the power flow trend in distribution systems such that

power flow was mostly one directional, namely from transmission to distribution, however now it flows in and out of a distribution system, even it circulates inside the system. Hybrid grid configuration brings some benefits with it like [8]:

- Conversion loss is minimized since some AC/DC conversion stages are removed.
- More simple and cost effective electronic products can be made by getting rid of redundant DC rectifiers.
- AC side power quality is increased since harmonic injections can be controlled through converter which connects DC side with all DC loads are connected.

As the electricity generation sources diversify, the integration of distributed generations to the existent central generation and grid management is going to require operations that are more resilient. Thanks to decentralized energy management system concepts, which one of them is shown in Figure 12, operations to establish a balance between load side and distributed generation side are not going to be a difficult task.

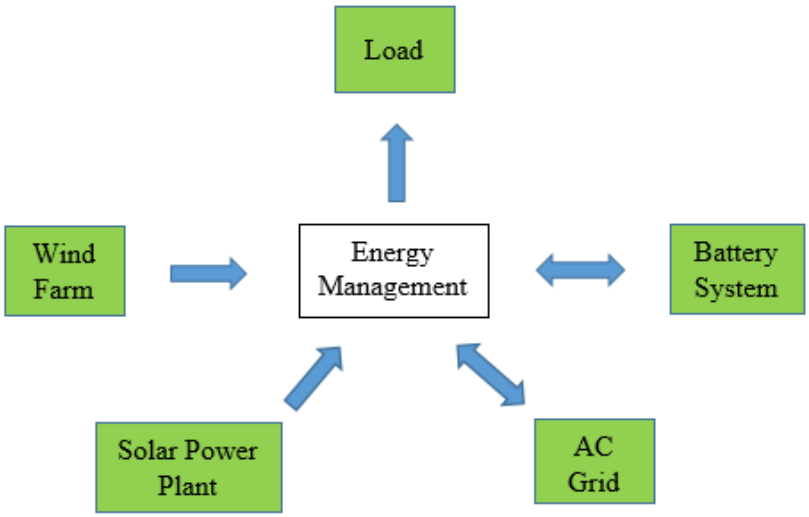

Figure 12. A Decentralized Energy Management System Concept

New communication network infrastructures with sensors and monitoring devices, automation tools are going to provide a comprehensive understanding of the system situation [21]. In line with these requirements and recent developments in the power electronics field, existing grid is undergoing a change towards a more digital and intelligent one as shown in Table 2. All of these require a new and more intelligent grid concept. Intelligent grid that utilizes new type of electricity generation sources, information technologies, sensors and monitoring devices to collect necessary data in order to create a more integrated and smart environment for all players in the electricity business is called Smart Grid [22].

Table 2. Existing Grid vs. Smart Grid [22]

Existing Grid	**Smart Grid**
Unidirectional	Bidirectional
Electromechanic	More Digital
Centralized	Distributed
Few Sensors	Plenty of Sensors
Manual Control	Automatic/Self-Healing
Local Check/Test	Remote Check/Test
Limited Customer Choices	Many Customer Choices

Communication terminals and smart meters are used in smart grids to collect and exchange data about bus voltage, current and power supply or demand information with high-speed networks. Besides, it contributes to the existent system wellbeing by generating appropriate commands for taking necessary actions before a failure occurs and lowers financial expenditures. Through the use of management and communication tools, smart grids help to overcome the system complexity and to preserve the system in reliable conditions.

Although AC or DC Smart Grids are studied before, Smart Grids for the concept of hybrid systems incorporating both AC and DC grids are a recent concern [23]. To be able to increase the system reliability and to ensure uninterrupted supply for sensitive loads, the DC grid, which has connection to storage systems and distributed generators, is combined with the AC grid by converters. The configuration presented in [23], incorporates centralized control systems for AC and DC microgrids. AC systems have already installed wind turbines with AC/DC/AC converters and solar power systems with DC to AC inverters. A battery storage system is connected together with distributed generators because sometimes these type of generators cannot supply enough power resulting in undesired voltage and frequency abnormalities. Along with battery storage systems, EV charging stations are also connected to the AC network through AC/DC converters. However, AC/DC/AC converters of turbine generators and AC/DC converters of battery storage systems and EV charging stations are replaced with cheaper DC/DC converters in the DC side.

Smart Grid control systems gather necessary data and modulates PWM signal of the converters according to measurements collected off the system to ensure the grid is in a safe condition. Loads connected to DC side are supplied through local distributed generators and if power supply is not adequate, then AC side supports the deficit. DC side can continue to its operations when a fault on the AC side occurs or even it can supply power to the AC side. A representative topology is given in Figure 13. Following benefits may be expected in this kind of hybrid configuration [23]:

- In case of electricity shortages, battery storage systems step in and provide continuous power to sensitive loads.

- AC side waveform distortion problems can be encountered due to presence of AC/DC converters; however, DC loads may have a direct connection to a DC bus in a hybrid structure thus eliminating some AC/DC converters.

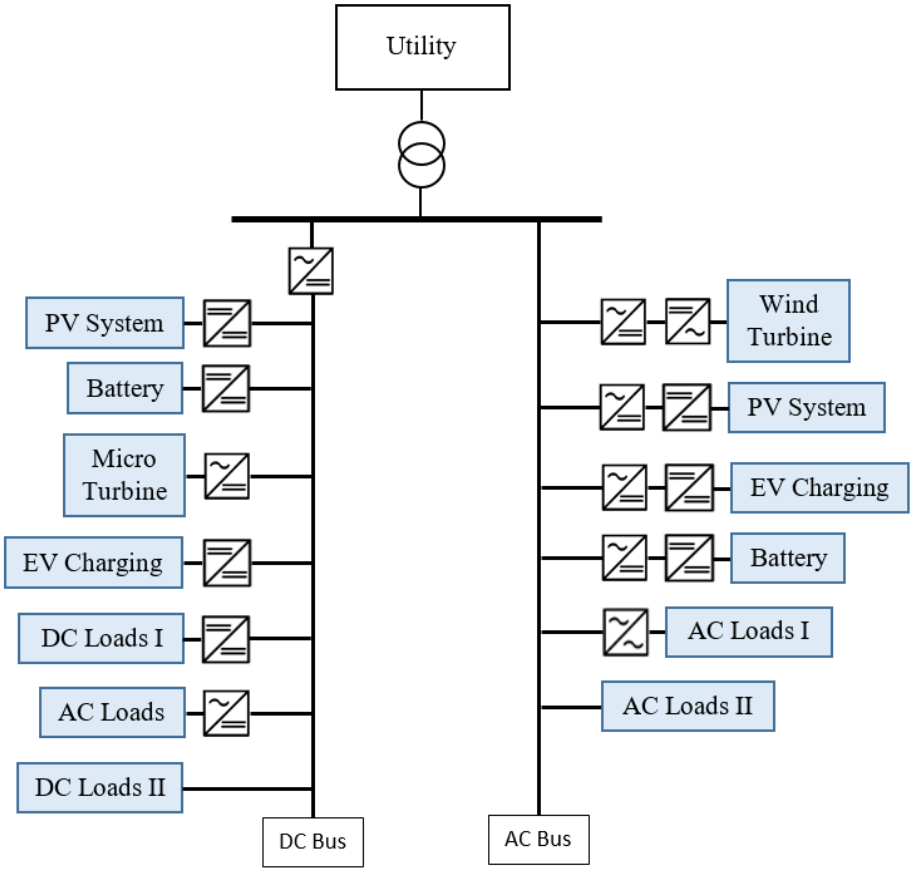

Figure 13. A Representative Topology for an AC/DC Smart Grid

2.5 Literature review on Hybrid Smart Grids and AC/DC Load Flow

Renewable generations have gained a significant place in the last decade with the rising trend to abandon fossil fuel based electricity generation. Utilization of these renewable distributed generators in the low voltage network resulted in a more decentralized power system and it has brought many advantages to both the consumers and distribution system [24].

Not only the trend was changing in the generation side, loads have also evolved with the advancement in electronics and it is shown that DC distribution system can

supply most of the loads in offices or commercial facilities in a more efficient way [25]. Study in [26] stated that as power electronics field develops, home appliances can be modified for integration into DC network and DC supply can help to reduce power consumption of these appliances resulting in a better overall system efficiency.

In another study, how critical devices in hospitals, banks or other commercial buildings may get benefit from a DC distribution system is studied and it is indicated that these systems are more favourable compared to AC systems when supplying sensitive loads [27]. Even a prototype DC house is designed as an alternative for a common AC house system [28]. Another study that compares DC distribution against AC distribution has stated that EV charging stations can also get benefit of faster charging ability with higher voltage levels of DC grids [29].

Some other comprehensive works have been done on DC grids regarding their interconnection to AC network, how power quality is affected, standardization and protection issues as well as different implementation topologies [30], [31]. Since the traditional electrical system is an AC dominant structure, transition to completely DC network is not going to be immediate, but will be a smoother one with the adaption of DC grids constituting a hybrid one [32]. Another study also focused on economic aspects of AC/DC distribution systems and a planning method is proposed for these systems [33]. Researches in [34] showed that hybrid smart AC/DC systems can get benefits of AC and DC systems.

Although various researches have been conducted on AC and DC network topologies, how to analyse load flow on these new type of hybrid AC/DC and smart distribution systems stayed on the sidelines. Some studies have been presented on power flow analysis of HVDC systems.

There are basically two kind of methods for the load flow problem of AC/DC systems that are unified and sequential approaches. The unified method interprets AC and DC equations together whereas they are solved separately in the sequential method. Research in [35] presented a VSC model with mathematical expressions

to be used for hybrid multi-terminal AC/DC distribution network sequential load flow algorithm and it is stated that converter modelling has an important role in the power flow study and converter losses have significant impact on the load flow results. Another study focused on the effects of converter outages and faults on steady state conditions of AC/DC hybrid systems by implementing a sequential method [36].

Researches of [2] and [3] presented a unified method to be used in AC systems with HVDC transmission networks incorporating multi-terminal voltage-source converter (VSC). In those studies, it is indicated that high number of iterative loops in a sequential method results in a complicated algorithm and requires more time to converge to a solution compared to a unified method. Researchers of [37] developed a modified sequential AC/DC load flow analysis approach and Newton-Raphson iteration is used to solve DC equations and mentioned approach is implemented in China Southern Grid. This study indicated that sequential method may have severe problems in some cases and may result in solutions that are not feasible in terms of converter parameters, may have interruptions and failures. Other than that, a VSC model for sequential load flow method is presented in detail in [38]. Again, researchers proposed power flow algorithm using equivalent injected power method and created mathematical expression for VSC based HVDC system in [39].

In another study, the sequential algorithm performance is compared to simultaneous algorithm for VSC based HVDC transmission system and Newton-Raphson iteration is implemented to solve AC and DC equations [40]. In [41], it is aimed to analyse optimal load flow problem for an AC network incorporating many DC grids to reduce the network electricity generation total cost and the solution is calculated by changing the AC/DC load flow problem to an AC load flow problem and using semidefinite program relaxation technique. In the previously mentioned studies, AC and DC grids have their own respective equations which are convenient for HVDC systems, whereas research presented in [1] proposes an AC and DC combined equations for hybrid AC/DC distribution networks.

CHAPTER 3

SYSTEM DESCRIPTION AND CONVERTER MODELS

To be able to determine steady state conditions of an electrical power network, load flow analysis is applied. Interconnecting nodes, branches, load and generator data are used to obtain a power system model and this helps to evaluate operating state of a power system under given characteristics. Thanks to the load flow analysis, possible problems can be predicted before a contingency occurs and thus, reliable power system operation can be maintained. Load flow study also helps to plan future network expansions and economical operations.

At the beginning of this chapter, system bus classification is given and converter models are provided. Since equations used in this analysis are non-linear, Newton-Raphson method is used and its application to an ordinary AC system is presented. Later, derivation procedure of the modified Jacobian matrix for an AC/DC hybrid system is explained.

3.1 Description of System Buses and Converter Types

AC/DC distribution networks include different combinations of AC and DC buses. For AC buses, there are three categories [42]:

1. AC Slack Bus: This is the reference bus that the voltage magnitude and the phase angle (θ) values are known initially. Active (P) and reactive (Q) powers are variables and they are unknown at the beginning.
2. PQ Bus: This is the AC load bus for which active and reactive powers consumed by connected loads are known but phase angle and voltage magnitude are not known for this type of buses.

3. PV Bus: This is the AC generator bus. Generated active power and magnitude of the voltage are known, however phase angle and generated reactive power values are variable.

For the DC Buses, voltage magnitude and active power values are two basic parameters. There are two types of DC buses [1]:

1. DC Generator (V^{DC}) Bus: This is the generator bus that the voltage magnitude is known, but net active power injected is not known.
2. DC Load (P^{DC}) Bus: This is the bus that net active power is known but voltage magnitude is unknown.

Known and unknown parameters are shown according to bus types in Table 3. A tick means the parameter is known whereas a cross means the parameter is unknown. Note that reactive power and phase angle are not an interest for a DC bus. VSCs are used at the interfacing buses of AC and DC grids and DC/DC converters are utilized to have a control over DC bus voltages. Three different DC/DC converter types and one AC/DC converter model are presented in this section; however, any converter model can be implemented using the same procedure defined in here as long as the voltage transfer equation of the converter is known.

Table 3. AC and DC Bus Parameters.

Bus Type	**V**	**θ**	**P**	**Q**
AC Slack Bus	✓	✓	X	X
AC PV Bus	✓	X	✓	X
AC PQ Bus	X	X	✓	✓
Vdc Bus	✓	-	X	-
Pdc Bus	X	-	✓	-

3.1.1 DC/DC Buck Converter Model

This converter produces an output voltage lower than the converter supply voltage. It is widely used in power supply circuits of electronic devices and dc motor drive applications. It is also called a step-down converter. Converter output voltage is adjusted by changing the duty ratio (D) which is calculated by dividing "on" duration of the switch to the switching period and it is always less than "1". The expression for a buck converter model is [43]:

$$V_{out} = DV_{in} \tag{1}$$

3.1.2 DC/DC Boost Converter Model

Output terminal voltage of this converter is greater than the converter supply voltage. It is utilized in power supply circuits of electronic devices and regenerative braking of dc motor applications. The converter allows controlling its output voltage by varying the duty ratio. This converter is also known as a step-up converter and the equation for this converter model is [43]:

$$V_{out} = \frac{V_{in}}{1 - D} \tag{2}$$

3.1.3 DC/DC Buck-Boost Converter Model

This converter is formed by cascading buck and boost converters. Therefore, it may have a voltage output greater or lower than the converter supply voltage level. The transfer expression for a buck-boost converter model is [43]:

$$V_{out} = \frac{DV_{in}}{1 - D} \tag{3}$$

3.1.4 AC/DC Converter Model

To be able to obtain an AC voltage from a DC source, a voltage source converter (VSC) is utilized. VSC is a bidirectional device allowing current reversal thus enabling power exchange within the system and it is used for AC/DC conversion in this study. AC and DC terminal voltages of this converter are related by the modulation index (M) and the it is expressed using the following equation [44]:

$$V_{pu}^{AC} = MV_{pu}^{DC} \tag{4}$$

3.2 Power Flow Equations and Newton-Raphson Method

To determine the operating state of an electrical power system, load flow analysis is performed and power flow equations can be obtained with the procedure as defined in [42]**.** Now let $\boldsymbol{V_n}$ and $\boldsymbol{I_n}$be the phasor voltage and current at bus n

$$\begin{aligned} \boldsymbol{V_n} &= V_n e^{j\theta_n} \\ \theta_{nm} &= \theta_n - \theta_m \\ Y_{nm} &= G_{nm} + jB_{nm} \end{aligned} \tag{5}$$

For an AC system, injected current at bus n is

$$\boldsymbol{I_n} = \left(\sum_{m=1}^{N_{Bus}} Y_{nm} \boldsymbol{V_m} \right) \tag{6}$$

Then, injected complex power at bus n becomes

$$\begin{aligned} S_n &= \boldsymbol{V_n I_n^*} \\ &= \boldsymbol{V_n}\left(\sum_{m=1}^{N_{Bus}} Y_{nm}^* \boldsymbol{V_m^*}\right) \end{aligned} \tag{7}$$

Using (5) in (7) gives that

$$\begin{aligned} S_n &= \sum_{m=1}^{N_{Bus}} V_n V_m e^{j\theta_{nm}}(G_{nm} - jB_{nm}) \\ &= \sum_{m=1}^{N_{Bus}} V_n V_m (cos\theta_{nm} + jsin\theta_{nm})(G_{nm} - jB_{nm}) \end{aligned} \tag{8}$$

Equation (8) can be resolved into real and imaginary parts to have active and reactive power equations

$$\begin{aligned} P_n &= \sum_{m=1}^{N_{Bus}} V_n V_m (G_{nm} cos\theta_{nm} + B_{nm} sin\theta_{nm}) \\ Q_n &= \sum_{m=1}^{N_{Bus}} V_n V_m (G_{nm} sin\theta_{nm} - B_{nm} cos\theta_{nm}) \end{aligned} \tag{9}$$

Now, suppose there are n nonlinear set of functions $F(x) = 0$, roots x at k^{th} iteration which is an $nx1$ vector can be obtained by utilizing Taylor Series [42]

$$x^{k+1} = x^k - [J(x^k)]^{-1} F(x^k) \tag{10}$$

where nxn Jacobian matrix is

$$J(x) = \begin{bmatrix} \frac{dF_1}{dx_1} & \cdots & \frac{dF_1}{dx_n} \\ \vdots & \ddots & \vdots \\ \frac{dF_n}{dx_1} & \cdots & \frac{dF_n}{dx_n} \end{bmatrix} \quad (11)$$

Then, rearranging (10) gives

$$\Delta x^k = x^{k+1} - x^k = -[J^k]^{-1} F(x^k) \quad (12)$$

After finding Δx^k, one can proceed to next iteration with (13) and this iterative procedure is applied until the convergence is reached.

$$x^{k+1} = x^k + \Delta x^k \quad (13)$$

Newton-Raphson iterative solution procedure can be applied to power flow equations as well. First, implementation of Newton-Raphson iteration in an AC system is going to be explained and afterwards it is going to be extended for a hybrid AC/DC system.

3.2.1 Implementation for an AC System

For an AC system, voltage magnitude and phase angle of the slack bus are known and hence it is skipped in the iterative process. Unless reactive limit of a generator bus is violated, PV bus voltage magnitude is specified and hence, no need to take it

as an unknown. Therefore, V and θ are unknowns for a PQ bus and only θ is an unknown for a PV bus, so there are $2N_{PQ} + N_{PV}$ unknowns. If bus 1 is assumed as the slack bus, the unknown vector x can be defined as

$$x = \begin{bmatrix} \theta_2 \\ \vdots \\ \theta_i \\ V_2 \\ \vdots \\ V_r \end{bmatrix} \quad \text{for} \quad \begin{matrix} i, r = 2, 3, \dots, N_{Bus} \\ r \neq PV \end{matrix} \tag{14}$$

Solution procedure starts with an initial guess such that "1.0 p.u." for voltage magnitudes and "0 degrees" for phase angles are assigned. Then, using the assigned values of x, injected active and reactive power functions, $P_n(x)$ and $Q_n(x)$ respectively, can be evaluated as [42]

$$\begin{aligned} P_n(x) &= \sum_{m=1}^{N_{Bus}} V_n V_m (G_{nm} cos\theta_{nm} + B_{nm} sin\theta_{nm}) \\ Q_n(x) &= \sum_{m=1}^{N_{Bus}} V_n V_m (G_{nm} sin\theta_{nm} - B_{nm} cos\theta_{nm}) \end{aligned} \tag{15}$$

Note that functions in (15) are evaluated using the unknown vector x and they are going to be referred as

$$\begin{aligned} P_n^{calc} &= P_n(x) \\ Q_n^{calc} &= Q_n(x) \end{aligned} \tag{16}$$

Reactive power limit for each generator bus should be checked at each iteration. A generator bus is regarded as a PV bus only if reactive power generation stays within limits. If a reactive power limit is reached, a PV bus is changed to a PQ bus with a reactive power injection equals to the violated limit.

If this is the case, then the voltage magnitude of that bus appears as a variable in the unknown vector and the mismatch vector and Jacobian matrix are modified accordingly.

$$\begin{aligned} &\text{If} \quad Q_G > Q_G^{max}, \qquad Q_G = Q_G^{max} \\ &\text{If} \quad Q_G < Q_G^{min}, \qquad Q_G = Q_G^{min} \end{aligned} \tag{17}$$

After continuing with next iterations, if reactive power generation of a PQ bus, which was formerly a PV bus, falls in limits, this time bus type changes from PQ to PV again with a fixed voltage magnitude. Next, specified powers are calculated with the following equation (18)

$$\begin{aligned} P_n^{spec} &= P_n^{G,AC} - P_n^{L,AC} \\ Q_n^{spec} &= Q_n^{G,AC} - Q_n^{L,AC} \end{aligned} \tag{18}$$

Now, aim is to match specified powers with the calculated ones as in (19)

$$\begin{aligned} P_n^{spec} &= P_n^{calc} \\ Q_n^{spec} &= Q_n^{calc} \end{aligned} \tag{19}$$

If equations in (19) can be arranged in the form $F(x) = 0$, it becomes

$$F(x) = \begin{bmatrix} P_2^{spec} - P_2^{calc} \\ \vdots \\ P_i^{spec} - P_i^{calc} \\ Q_2^{spec} - Q_2^{calc} \\ \vdots \\ Q_r^{spec} - Q_r^{calc} \end{bmatrix} \quad \text{for} \quad \begin{matrix} i, r = 2, 3, \dots, N_{Bus} \\ r \neq PV \end{matrix} \tag{20}$$

This constitutes a power mismatch vector denoted in (21)

$$F(x) = \begin{bmatrix} \Delta P_2 \\ \vdots \\ \Delta P_i \\ \Delta Q_2 \\ \vdots \\ \Delta Q_r \end{bmatrix} \quad \text{for} \quad \begin{matrix} i, r = 2, 3, \dots, N_{Bus} \\ r \neq PV \end{matrix} \tag{21}$$

where

$$\begin{aligned} \Delta P_n &= P_n^{spec} - \sum_{m=1}^{N_{Bus}} V_n V_m (G_{nm} cos\theta_{nm} + B_{nm} sin\theta_{nm}) \\ \Delta Q_n &= Q_n^{spec} - \sum_{m=1}^{N_{Bus}} V_n V_m (G_{nm} sin\theta_{nm} - B_{nm} cos\theta_{nm}) \end{aligned} \tag{22}$$

Here note that ΔP_n is defined for each PV and PQ bus whereas ΔQ_n is defined for only PQ buses. So there are $2N_{PQ} + N_{PV}$ power mismatch equations. Now, aim is to drive these mismatch equations to zero and Newton-Raphson iteration is utilized. Rearranging (12) gives

$$F(x^k) = [J^k]\Delta x^k \tag{23}$$

For k[th] iteration, using (14) and (21) in (23) leads to

$$\begin{bmatrix} \Delta P_2 \\ \vdots \\ \Delta P_i \\ \Delta Q_2 \\ \vdots \\ \Delta Q_r \end{bmatrix}^k = [J^k] \begin{bmatrix} \Delta \theta_2 \\ \vdots \\ \Delta \theta_i \\ \Delta V_2 \\ \vdots \\ \Delta V_r \end{bmatrix}^k \quad \text{for} \quad \begin{matrix} i, r = 2, 3, \dots, N_{Bus} \\ r \neq PV \end{matrix} \tag{24}$$

and Jacobian matrix is

$$J^k = \begin{bmatrix} J^1 & J^2 \\ J^3 & J^4 \end{bmatrix}^k \tag{25}$$

where

$$\begin{aligned} J_{nm}^1 &= \frac{dP_n(x)}{d\theta_m} \\ J_{nm}^2 &= \frac{dP_n(x)}{dV_m} \\ J_{nm}^3 &= \frac{dQ_n(x)}{d\theta_m} \\ J_{nm}^4 &= \frac{dQ_n(x)}{dV_m} \end{aligned} \tag{26}$$

After obtaining Δx^k, convergence is checked with a prespecified power mismatch threshold ε .

$$\text{If} \qquad \max \left| \begin{matrix} \Delta P_n \\ \Delta Q_n \end{matrix} \right|^k < \varepsilon \tag{27}$$

solution converges and iterations stop. If this is not the case, iteration continues with the updated x vector until the mismatch criterion is satisfied.

3.2.2 Implementation for an AC/DC System

Previously given equations for an AC system are extended so that they include DC equations together with unknown duty ratios and modulation indexes for converters operating in constant voltage mode for a hybrid AC/DC system. Here, another classification is introduced for constant voltage controlled buses.

If a PQ bus is voltage controlled, it is going to be denoted as ACCV and M is the unknown instead of the voltage magnitude. If a DC load bus is voltage controlled, it is going to be denoted as DCCV and duty ratio is the unknown instead of the voltage magnitude. Table 4 summarizes the unknown parameters.

Table 4. Unknown Variables for an AC/DC Hybrid System

Bus Type	Unknowns
AC PQ Bus	V and θ
AC PV Bus	θ
DC Load Bus	V
ACCV Bus	M and θ
DCCV Bus	D

There is no unknown for a DC Generator (V^{DC}) Bus. Then, the unknown vector x becomes

$$x = \begin{bmatrix} \theta_n \\ \vdots \\ V_h \\ \vdots \\ V_i \\ \vdots \\ M_p \\ \vdots \\ D_r \\ \vdots \end{bmatrix} \quad \text{for} \quad \begin{matrix} \forall n \in \text{PV, PQ, ACCV} \\ \\ \forall h \in \text{PQ} \\ \\ \forall i \in \text{DC Load} \\ \\ \forall p \in \text{ACCV} \\ \\ \forall r \in \text{DCCV} \end{matrix} \tag{28}$$

Figure 14 illustrates possible load and generator connections in an AC/DC system. DC generators and loads may have a connection to an AC bus and AC generators and loads may also have a connection to a DC Bus by utilizing AC/DC converters.

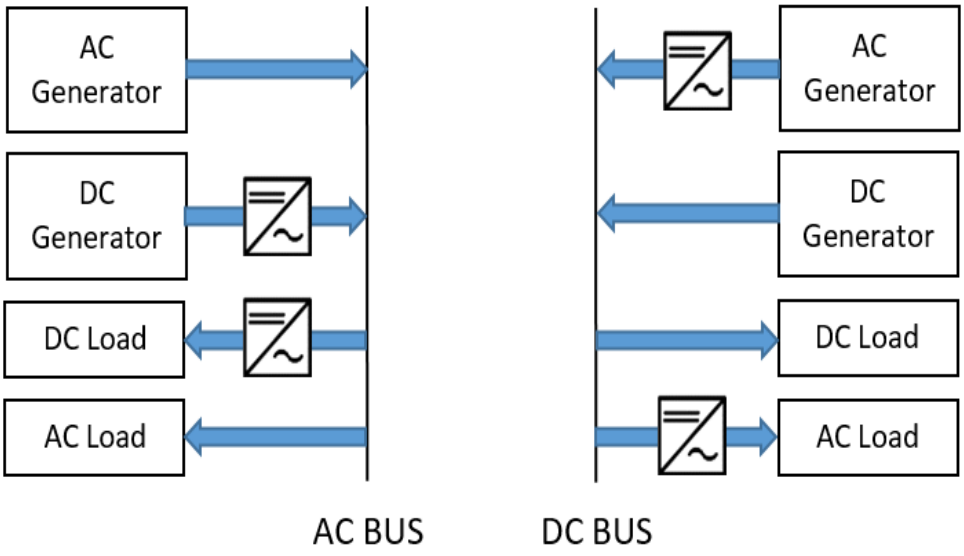

Figure 14. Generator and Load Connections for Different Bus Types

Specified power relations can be obtained according to connection types. If a generator or load is connected to a bus through a converter, then power loss due to power converter efficiency should be accounted with the following equations [1]

$$P_n^{spec} = P_n^{G,AC} - P_n^{L,AC} + \eta P_n^{G,DC} - \frac{P_n^{L,DC}}{\eta} \quad \text{, if n is an AC Bus}$$
$$Q_n^{spec} = Q_n^{G,AC} - Q_n^{L,AC} + Q_n^{G,DC} - Q_n^{L,DC} \qquad (29)$$
$$P_n^{spec} = P_n^{G,DC} - P_n^{L,DC} + \eta P_n^{G,AC} - \frac{P_n^{L,AC}}{\eta} \quad \text{, if n is a DC Bus}$$

Power mismatches are

$$\Delta P_n = P_n^{spec} - P_n^{calc}$$
$$\Delta Q_n = Q_n^{spec} - Q_n^{calc} \qquad (30)$$

Mismatch vector for an AC/DC hybrid system is defined as

$$F(x) = \begin{bmatrix} \Delta P_n \\ \vdots \\ \Delta Q_h \\ \vdots \\ \Delta P_i \\ \vdots \\ \Delta Q_p \\ \vdots \\ \Delta P_r \\ \vdots \end{bmatrix} \quad \begin{matrix} \forall \text{n} \in \text{PV, PQ, ACCV} \\ \\ \forall \text{h} \in \text{PQ} \\ \\ \forall \text{i} \in \text{DC Load} \\ \\ \forall \text{p} \in \text{ACCV} \\ \\ \forall \text{r} \in \text{DCCV} \end{matrix} \tag{31}$$

Now using (28) and (31) in (23) gives

$$\begin{bmatrix} \Delta P_n \\ \vdots \\ \Delta Q_h \\ \vdots \\ \Delta P_i \\ \vdots \\ \Delta Q_p \\ \vdots \\ \Delta P_r \\ \vdots \end{bmatrix} = \begin{bmatrix} J^1 & J^2 & J^5 & J^{10} \\ J^3 & J^4 & J^6 & J^{11} \\ J^7 & J^8 & J^9 & J^{12} \\ J^{13} & J^{14} & J^{15} & J^{16} \end{bmatrix} \begin{bmatrix} \Delta \theta_n \\ \vdots \\ \Delta \text{V}_h \\ \vdots \\ \Delta \text{V}_i \\ \vdots \\ \Delta M_p \\ \vdots \\ \Delta D_r \\ \vdots \end{bmatrix} \tag{32}$$

For hybrid systems, in addition to the reactive power limits of PV buses, active power limits for DC generator buses should be checked at each iteration. For convenience, Equation 17 is repeated here

$$\begin{matrix} \text{If} \quad Q_G > Q_G^{max}, & Q_G = Q_G^{max} \\ & \text{for PV Buses} \\ \text{If} \quad Q_G < Q_G^{min}, & Q_G = Q_G^{min} \end{matrix} \tag{17}$$

A DC generator bus maintains specified voltage if calculated active power is within limits of the generator. If active power limit is violated, type of the DC generator bus changes to a DC load bus and active power is maintained at that limit. The bus voltage magnitude in this case appears as a variable in the unknown vector.

$$\text{If} \quad P_G > P_G^{max}, \qquad P_G = P_G^{max}$$
$$\text{If} \quad P_G < P_G^{min}, \qquad P_G = P_G^{min} \qquad \text{for DC Generator Buses} \quad (33)$$

After continuing with next iterations, those DC load buses which were formerly DC generator buses are checked. If active power generation of a DC load bus falls within limits, bus type is changed back to DC generator bus again.

Now, Jacobian matrix is going to be investigated in more detail. First of all, J^1 is a $(N_{PV} + N_{PQ} + N_{ACCV})x(N_{PV} + N_{PQ} + N_{ACCV})$ matrix and it is the derivative of PV, PQ and ACCV bus active powers with respect to voltage angles.

$$J_{nm}^1 = \frac{dP_n}{d\theta_m}, \qquad \forall \text{n, m} \in (N_{PV} + N_{PQ} + N_{ACCV}) \qquad (34.1)$$

J^2 is a $(N_{PV} + N_{PQ} + N_{ACCV})x(N_{PQ} + N_{DCL})$ matrix and it is the derivative of PV, PQ and ACCV bus active powers with respect to PQ and DC load bus voltage magnitudes.

$$J_{nm}^2 = \frac{dP_n}{dV_m}, \qquad \begin{matrix} \forall \text{n} \in (N_{PV} + N_{PQ} + N_{ACCV}) \\ \forall \text{m} \in (N_{PQ} + N_{DCL}) \end{matrix} \qquad (34.2)$$

J^3 is a $(N_{PQ} + N_{DCL})x(N_{PV} + N_{PQ} + N_{ACCV})$ matrix and it is the derivative of PQ bus reactive powers and DC load bus active powers with respect to voltage angles.

$$J_{nm}^3 = \begin{cases} \dfrac{dQ_n}{d\theta_m}, & \forall \text{n} \in N_{PQ}, \forall \text{m} \in (N_{PV} + N_{PQ} + N_{ACCV}) \\ 0, & \forall \text{n} \in N_{DCL} \end{cases} \qquad (34.3)$$

J^4 is a $(N_{PQ} + N_{DCL})x(N_{PQ} + N_{DCL})$ matrix and it is the derivative of PQ bus reactive powers and DC load bus active powers with respect to PQ and DC load bus voltage magnitudes.

$$J_{nm}^{4} = \begin{cases} \dfrac{dQ_n}{dV_m}, & \forall \mathrm{n} \in N_{PQ}, \forall \mathrm{m} \in (N_{PQ} + N_{DCL}) \\ \dfrac{dP_n}{dV_m}, & \forall \mathrm{n} \in N_{DCL}, \forall \mathrm{m} \in (N_{PQ} + N_{DCL}) \end{cases} \tag{34.4}$$

J^5 is a $(N_{PV} + N_{PQ} + N_{ACCV})x(N_{ACCV})$ matrix and it is the derivative of PV, PQ and ACCV bus active powers with respect to modulation indexes of converters which are connected to ACCV buses.

$$J_{nm}^{5} = \frac{dP_n}{dM_m}, \qquad \begin{matrix} \forall \mathrm{n} \in (N_{PV} + N_{PQ} + N_{ACCV}) \\ \forall \mathrm{m} \in (N_{ACCV}) \end{matrix} \tag{34.5}$$

J^6 is a $(N_{PQ} + N_{DCL})x(N_{ACCV})$ matrix and it is the derivative of PQ bus reactive powers and DC load bus active powers with respect to modulation indexes of converters which are connected to ACCV buses.

$$J_{nm}^{6} = \begin{cases} \dfrac{dQ_n}{dM_m}, & \forall \mathrm{n} \in N_{PQ}, \forall \mathrm{m} \in (N_{ACCV}) \\ \dfrac{dP_n}{dM_m}, & \forall \mathrm{n} \in N_{DCL}, \forall \mathrm{m} \in (N_{ACCV}) \end{cases} \tag{34.6}$$

J^7 is a $(N_{ACCV})x(N_{PV} + N_{PQ} + N_{ACCV})$ matrix and it is the derivative of ACCV bus reactive powers with respect to PV, PQ and ACCV bus voltage angles.

$$J_{nm}^{7} = \frac{dQ_n}{d\theta_m}, \qquad \begin{matrix} \forall \mathrm{n} \in (N_{ACCV}) \\ \forall \mathrm{m} \in (N_{PV} + N_{PQ} + N_{ACCV}) \end{matrix} \tag{34.7}$$

J^8 is a $(N_{ACCV})x(N_{PQ} + N_{DCL})$ matrix and it is the derivative of ACCV bus reactive powers with respect to PQ and DC load bus voltage magnitudes.

$$J_{nm}^{8} = \frac{dQ_n}{dV_m}, \qquad \begin{matrix} \forall \mathrm{n} \in (N_{ACCV}) \\ \forall \mathrm{m} \in (N_{PQ} + N_{DCL}) \end{matrix} \tag{34.8}$$

J^9 is a $(N_{ACCV})x(N_{ACCV})$ matrix and it is the derivative of ACCV bus reactive powers with respect to modulation indexes of converters which are connected to ACCV buses.

$$J_{nm}^{9} = \frac{dQ_n}{dM_m}, \qquad \forall \mathrm{n, m} \in (N_{ACCV}) \tag{34.9}$$

J^{10} is a $(N_{PV} + N_{PQ} + N_{ACCV})x(N_{DCCV})$ matrix and it is the derivative of PV, PQ and ACCV bus active powers with respect to duty ratios of converters which are connected to DCCV buses.

$$J_{nm}^{10} = \frac{dP_n}{dD_m}, \qquad \begin{matrix} \forall \mathrm{n} \in (N_{PV} + N_{PQ} + N_{ACCV}) \\ \forall \mathrm{m} \in (N_{DCCV}) \end{matrix} \tag{34.10}$$

J^{11} is a $(N_{PQ} + N_{DCL})x(N_{DCCV})$ matrix and it is the derivative of PQ bus reactive powers and DC load bus active powers with respect to duty ratios of converters which are connected to DCCV buses.

$$J_{nm}^{11} = \begin{cases} \dfrac{dQ_n}{dD_m}, & \forall \mathrm{n} \in N_{PQ}, \forall \mathrm{m} \in (N_{DCCV}) \\ \dfrac{dP_n}{dD_m}, & \forall \mathrm{n} \in N_{DCL}, \forall \mathrm{m} \in (N_{DCCV}) \end{cases} \tag{34.11}$$

J^{12} is a $(N_{ACCV})x(N_{DCCV})$ matrix and it is the derivative of ACCV bus reactive powers with respect to duty ratios of converters which are connected to DCCV buses.

$$J_{nm}^{12} = \frac{dQ_n}{dD_m}, \qquad \begin{matrix} \forall \mathrm{n} \in (N_{ACCV}) \\ \forall \mathrm{m} \in (N_{DCCV}) \end{matrix} \tag{34.12}$$

J^{13} is a $(N_{DCCV})x(N_{PV}+N_{PQ}+N_{ACCV})$ matrix and it corresponds to the derivative of DCCV bus active powers with respect to PV, PQ ACCV bus voltage angles and it is nothing but zero.

$$J_{nm}^{13}=0\,, \qquad \begin{matrix}\forall \mathrm{n}\ \in (N_{DCCV}) \\ \forall \mathrm{m} \in (N_{PV}+N_{PQ}+N_{ACCV})\end{matrix} \tag{34.13}$$

J^{14} is a $(N_{DCCV})x(N_{PQ}+N_{DCL})$ matrix and it is the derivative of DCCV bus active powers with respect to PQ and DC load bus voltage magnitudes.

$$J_{nm}^{14}=\frac{dP_n}{dV_m}, \qquad \begin{matrix}\forall \mathrm{n}\ \in (N_{DCCV}) \\ \forall \mathrm{m} \in (N_{PQ}+N_{DCL})\end{matrix} \tag{34.14}$$

J^{15} is a $(N_{DCCV})x(N_{ACCV})$ matrix and it is the derivative of DCCV bus active powers with respect to modulation indexes of converters which are connected to ACCV buses.

$$J_{nm}^{15}=\frac{dP_n}{dM_m}\,, \qquad \begin{matrix}\forall \mathrm{n}\ \in (N_{DCCV}) \\ \forall \mathrm{m} \in (N_{ACCV})\end{matrix} \tag{34.15}$$

J^{16} is a $(N_{DCCV})x(N_{DCCV})$ matrix and it is the derivative of DCCV bus active powers with respect to duty ratios of converters which are connected to DCCV buses.

$$J_{nm}^{16}=\frac{dP_n}{dD_m}, \qquad \forall \mathrm{n,m} \in (N_{DCCV}) \tag{34.16}$$

As is the case with AC load flow analysis, Jacobian matrix is composed of partial derivatives of active and reactive power functions with respect to system unknowns. On the other hand, since there is a possibility to have a bus connected to different type of buses with a variety of converters, instead of defining a general bus power injection $P_n(x)$ and $Q_n(x)$ as in (11), summation of line flows are considered and

their respective derivatives are combined. An example case is illustrated in Figure 15. For this kind of a situation, $P_1^{AC} = P_{12}^{AC} + P_{13}^{AC} + P_{14}^{AC}$ and $Q_1^{AC} = Q_{12}^{AC} + Q_{13}^{AC} + Q_{14}^{AC}$ are bus 1 power injections and if one wants to find the partial derivate of P_1 with respect to voltage magnitudes V_1, V_2, V_3 and V_4

$$\begin{aligned}
\frac{dP_1^{AC}}{dV_1} &= \frac{dP_{12}^{AC}}{dV_1} + \frac{dP_{13}^{AC}}{dV_1} + \frac{dP_{14}^{AC}}{dV_1} \\
\frac{dP_1^{AC}}{dV_2} &= \frac{dP_{12}^{AC}}{dV_2} + 0 + 0 \\
\frac{dP_1^{AC}}{dV_3} &= 0 + \frac{dP_{13}^{AC}}{dV_3} + 0 \\
\frac{dP_1^{AC}}{dV_4} &= 0 + 0 + \frac{dP_{14}^{AC}}{dV_4}
\end{aligned} \tag{35}$$

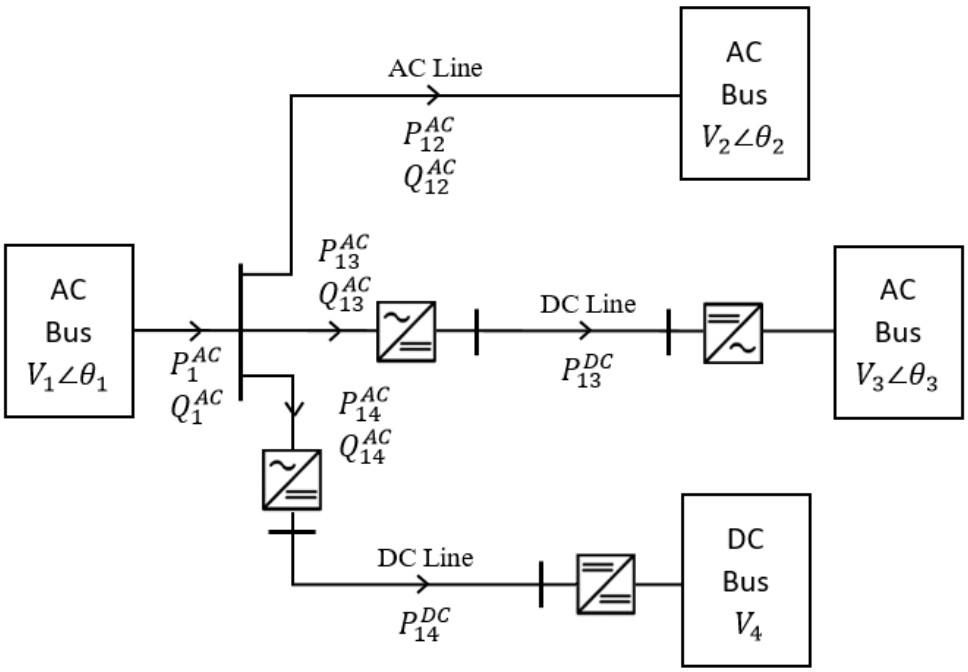

Figure 15. An AC Bus Connected to Different Busses

In a more general form, active and reactive power injections are

$$P_n^{calc} = \sum_{m=1}^{N_{Bus}} P_{nm} \quad \text{for m} \neq \text{n}$$
$$Q_n^{calc} = \sum_{m=1}^{N_{Bus}} Q_{nm} \quad \text{for m} \neq \text{n} \tag{36}$$

In short, when finding derivatives of these functions with respect to variables in the unknown vector x in order to use in Jacobian matrix, one can benefit from this summation also. The implementation of Newton-Raphson iterations in an AC/DC system is illustrated in Figure 16 below.

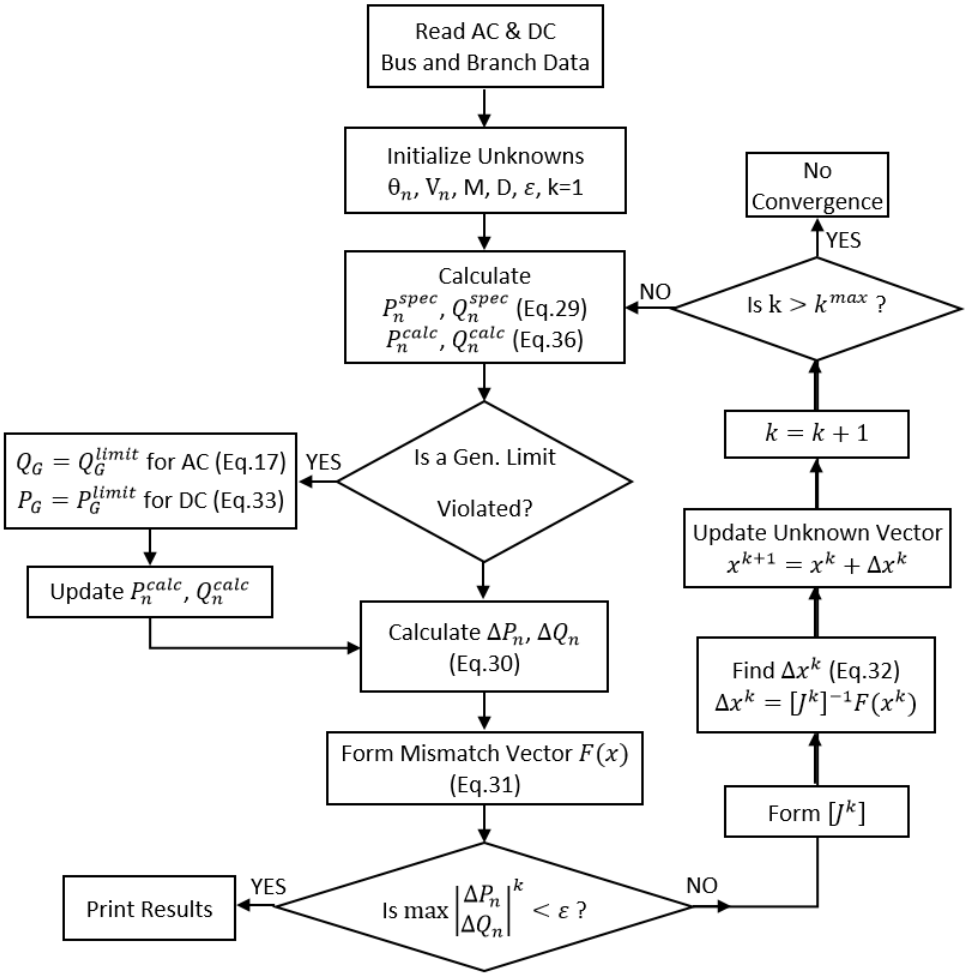

Figure 16. Flow Chart of the Presented Algorithm

3.3 Line Power Flows for Different Connection Types

Hybrid systems may include different combinations of AC and DC buses. In this part, power flow equations are given for various cases and partial derivatives which are used in Jacobian matrix are provided.

Case 1. AC Bus-AC Line-AC Bus

This case is illustrated in Figure 17. Line flow equations for active and reactive powers are as follows [1]

$$\begin{aligned} P_{nm} &= V_n^2 g_{nm} - V_n V_m (g_{nm} cos\theta_{nm} + b_{nm} sin\theta_{nm}) \\ Q_{nm} &= -V_n^2 b_{nm} - V_n V_m (g_{nm} sin\theta_{nm} - b_{nm} cos\theta_{nm}) \end{aligned} \tag{37}$$

Derivatives of line flow equations that are going to be used in Jacobian matrix are

$$\begin{aligned} \frac{dP_{nm}}{d\theta_n} &= -V_n V_m (-g_{nm} sin\theta_{nm} + b_{nm} cos\theta_{nm}) \\ \frac{dP_{nm}}{d\theta_m} &= -V_n V_m (g_{nm} sin\theta_{nm} - b_{nm} cos\theta_{nm}) \\ \frac{dP_{nm}}{dV_n} &= 2 * V_n * g_{nm} - V_m (g_{nm} cos\theta_{nm} + b_{nm} sin\theta_{nm}) \\ \frac{dP_{nm}}{dV_m} &= -V_n (g_{nm} cos\theta_{nm} + b_{nm} sin\theta_{nm}) \\ \frac{dQ_{nm}}{d\theta_n} &= -V_n V_m (g_{nm} cos\theta_{nm} + b_{nm} sin\theta_{nm}) \\ \frac{dQ_{nm}}{d\theta_m} &= V_n V_m (g_{nm} cos\theta_{nm} + b_{nm} sin\theta_{nm}) \\ \frac{dQ_{nm}}{dV_n} &= -2V_n b_{nm} - V_m (g_{nm} sin\theta_{nm} - b_{nm} cos\theta_{nm}) \\ \frac{dQ_{nm}}{dV_m} &= -V_n (g_{nm} sin\theta_{nm} - b_{nm} cos\theta_{nm}) \end{aligned} \tag{38}$$

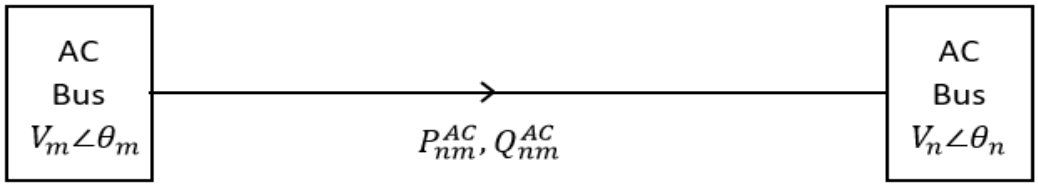

Figure 17. A Representative Schema for Case 1

Case 2. AC Bus-DC Line-AC Bus

Unlike the first case, this time an AC bus has a connection to another AC bus with a DC line and VSCs as shown in Figure 18. First, DC active power flow can be calculated as [1]

$$P_{nm}^{DC} = M_{nm}^{-1} V_n I_{nm}^{DC} \tag{39}$$

where

$$I_{nm}^{DC} = g_{nm} \left(M_{nm}^{-1} V_n - M_{mn}^{-1} V_m\right) \tag{40}$$

Also note that AC and DC side active powers are related with the converter efficiency depending on the power flow direction.

$$\begin{aligned} P_{nm}^{AC} &= P_{nm}^{DC} \frac{1}{\eta} && \text{if} \quad M_{nm}^{-1} V_n > M_{mn}^{-1} V_m \\ P_{nm}^{AC} &= P_{nm}^{DC} \eta && \text{if} \quad M_{nm}^{-1} V_n < M_{mn}^{-1} V_m \\ P_{nm}^{AC} &= P_{nm}^{DC} \left(\frac{0.5}{\eta} + 0.5\eta\right) && \text{if} \quad M_{nm}^{-1} V_n = M_{mn}^{-1} V_m \end{aligned} \tag{41}$$

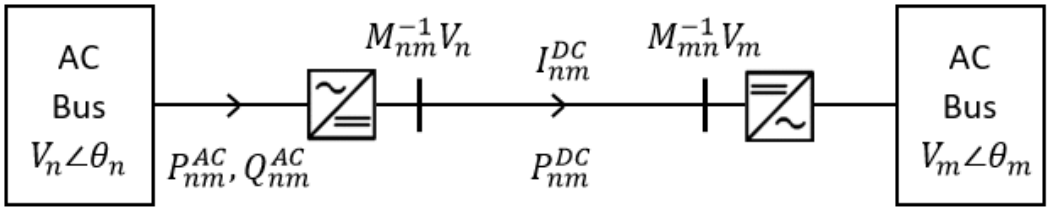

Figure 18. A Representative Schema for Case 2

After combining (39), (40) and (41) active and reactive power flows are calculated as (42), (43) and (44).

$$P_{nm} = g_{nm}\,(M_{nm}^{-2}V_n^2 - M_{nm}^{-1}V_n M_{mn}^{-1}V_m)(\frac{k_1}{\eta} + k_2\eta)$$
$$Q_{nm} = P_{nm}tan\varphi_{VSC} \quad (42)$$

where
$$k_1 = 1, \quad k_2 = 0 \quad \text{if} \quad M_{nm}^{-1}V_n > M_{mn}^{-1}V_m$$
$$k_1 = 0, \quad k_2 = 1 \quad \text{if} \quad M_{nm}^{-1}V_n < M_{mn}^{-1}V_m \quad (43)$$
$$k_1 = 0.5, \quad k_2 = 0.5 \quad \text{if} \quad M_{nm}^{-1}V_n = M_{mn}^{-1}V_m$$

Derivatives of line flow equations for Case 2 that are going to be used in Jacobian matrix are [1]

$$\frac{dP_{nm}}{d\theta_n} = 0, \quad \frac{dP_{nm}}{d\theta_m} = 0, \quad \frac{dQ_{nm}}{d\theta_n} = 0, \quad \frac{dQ_{nm}}{d\theta_m} = 0$$
$$\frac{dP_{nm}}{dV_n} = g_{nm}\,(M_{nm}^{-2} * 2V_n - M_{nm}^{-1}M_{mn}^{-1}V_m)(\frac{k_1}{\eta} + k_2\eta)$$
$$\frac{dQ_{nm}}{dV_n} = tan\varphi_{VSC} * \frac{dP_{nm}}{dV_n}$$
$$\frac{dP_{nm}}{dV_m} = g_{nm}\,(-M_{nm}^{-1}V_n M_{mn}^{-1})\left(\frac{k_1}{\eta} + k_2\eta\right)$$
$$\frac{dQ_{nm}}{dV_m} = tan\varphi_{VSC} * \frac{dP_{nm}}{dV_m} \quad (44)$$
$$\frac{dP_{nm}}{dM_{nm}} = g_{nm}\,(-2M_{nm}^{-3}V_n^2 + M_{nm}^{-2}V_n M_{mn}^{-1}V_m)\left(\frac{k_1}{\eta} + k_2\eta\right)$$
$$\frac{dQ_{nm}}{dM_{nm}} = tan\varphi_{VSC} * \frac{dP_{nm}}{dM_{nm}}$$
$$\frac{dP_{nm}}{dM_{mn}} = g_{nm}\,(M_{nm}^{-1}V_n M_{mn}^{-2}V_m)\left(\frac{k_1}{\eta} + k_2\eta\right)$$
$$\frac{dQ_{nm}}{dM_{mn}} = tan\varphi_{VSC} * \frac{dP_{nm}}{dM_{mn}}$$

Case 3. AC Bus-DC Line-DC Bus

In this configuration, an AC bus has a connection to a DC bus and they are connected with a DC line. VSC at AC bus converts AC voltage to DC as illustrated in Figure 19. Here, load flow equation is written from the AC side of the connection. Following same procedure described in Case 2

$$P_{nm}^{DC} = M_{nm}^{-1} V_n g_{nm} \left(M_{nm}^{-1} V_n - V_m\right) \tag{45}$$

AC side power flow equations are

$$\begin{aligned} P_{nm} &= g_{nm} \left(M_{nm}^{-2} V_n^2 - \left(M_{nm}^{-1} V_n V_m\right)\left(\frac{k_1}{\eta} + k_2 \eta\right)\right. \\ Q_{nm} &= P_{nm} tan\varphi_{VSC} \end{aligned} \tag{46}$$

where

$$\begin{aligned} &k_1 = 1, \quad k_2 = 0 \quad \text{if} \quad M_{nm}^{-1} V_n > V_m \\ &k_1 = 0, \quad k_2 = 1 \quad \text{if} \quad M_{nm}^{-1} V_n < V_m \\ &k_1 = 0.5, \quad k_2 = 0.5 \quad \text{if} \quad M_{nm}^{-1} V_n = V_m \end{aligned} \tag{47}$$

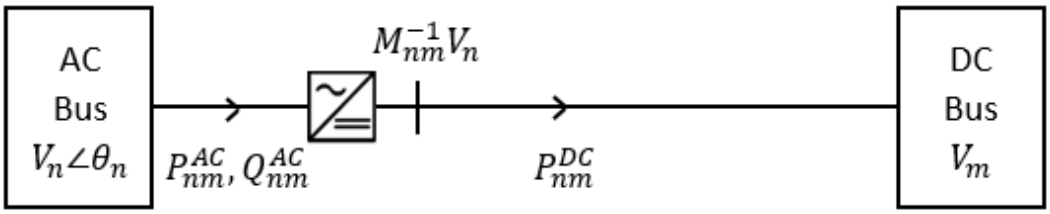

Figure 19. A Representative Schema for Case 3

Derivatives of line flow equations for Case 3 are

$$\begin{aligned}
\frac{dP_{nm}}{dV_n} &= g_{nm}\,(M_{nm}^{-2} * 2V_n - M_{nm}^{-1}V_m)(\frac{k_1}{\eta} + k_2\eta) \\
\frac{dQ_{nm}}{dV_n} &= tan\varphi_{VSC} * \frac{dP_{nm}}{dV_n} \\
\frac{dP_{nm}}{dV_m} &= g_{nm}\,(-M_{nm}^{-1}V_n)\left(\frac{k_1}{\eta} + k_2\eta\right) \\
\frac{dQ_{nm}}{dV_m} &= tan\varphi_{VSC} * \frac{dP_{nm}}{dV_m} \\
\frac{dP_{nm}}{dM_{nm}} &= g_{nm}\,(-2M_{nm}^{-3}V_n^2 + M_{nm}^{-2}V_nV_m)\left(\frac{k_1}{\eta} + k_2\eta\right) \\
\frac{dQ_{nm}}{dM_{nm}} &= tan\varphi_{VSC} * \frac{dP_{nm}}{dM_{nm}}
\end{aligned} \tag{48}$$

Case 4. AC Bus-DC Line–Buck-DC Bus

This case includes a DC/DC buck converter in addition to the configuration which is described in Case 3 as shown in Figure 20. Active power flow can be expressed as

$$P_{nm}^{DC} = M_{nm}^{-1}V_n g_{nm}\,(M_{nm}^{-1}V_n - D_{mn}^{-1}V_m) \tag{49}$$

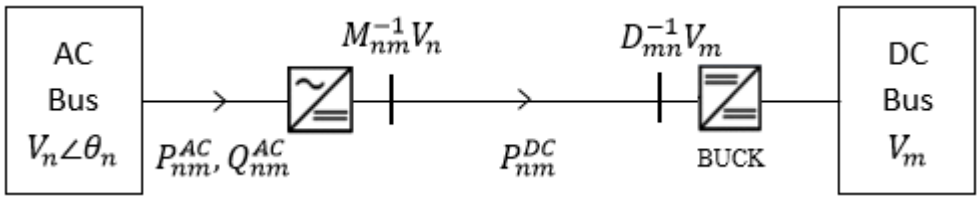

Figure 20. A Representative Schema for Case 4

AC side power flow equations are

$$\begin{aligned} P_{nm} &= g_{nm}\,(M_{nm}^{-2}V_n^2 - (M_{nm}^{-1}D_{mn}^{-1}V_nV_m)(\frac{k_1}{\eta} + k_2\eta) \\ Q_{nm} &= P_{nm}tan\varphi_{VSC} \end{aligned} \tag{50}$$

where

$$\begin{aligned} &k_1 = 1, \quad k_2 = 0 \quad \text{if} \quad M_{nm}^{-1}V_n > D_{mn}^{-1}V_m \\ &k_1 = 0, \quad k_2 = 1 \quad \text{if} \quad M_{nm}^{-1}V_n < D_{mn}^{-1}V_m \\ &k_1 = 0.5, \quad k_2 = 0.5 \quad \text{if} \quad M_{nm}^{-1}V_n = D_{mn}^{-1}V_m \end{aligned} \tag{51}$$

Derivatives of line flow equations for Case 4 are

$$\begin{aligned} \frac{dP_{nm}}{dV_n} &= g_{nm}\,(M_{nm}^{-2} * 2V_n - M_{nm}^{-1}D_{mn}^{-1}V_m)(\frac{k_1}{\eta} + k_2\eta) \\ \frac{dQ_{nm}}{dV_n} &= tan\varphi_{VSC} * \frac{dP_{nm}}{dV_n} \\ \frac{dP_{nm}}{dV_m} &= g_{nm}\,(-M_{nm}^{-1}D_{mn}^{-1}V_n)\left(\frac{k_1}{\eta} + k_2\eta\right) \\ \frac{dQ_{nm}}{dV_m} &= tan\varphi_{VSC} * \frac{dP_{nm}}{dV_m} \\ \frac{dP_{nm}}{dM_{nm}} &= g_{nm}\,(-2M_{nm}^{-3}V_n^2 + M_{nm}^{-2}D_{mn}^{-1}V_nV_m)\left(\frac{k_1}{\eta} + k_2\eta\right) \\ \frac{dQ_{nm}}{dM_{nm}} &= tan\varphi_{VSC} * \frac{dP_{nm}}{dM_{nm}} \\ \frac{dP_{nm}}{dD_{mn}} &= g_{nm}\,(M_{nm}^{-1}D_{mn}^{-2}V_nV_m)\left(\frac{k_1}{\eta} + k_2\eta\right) \\ \frac{dQ_{nm}}{dD_{mn}} &= tan\varphi_{VSC} * \frac{dP_{nm}}{dD_{mn}} \end{aligned} \tag{52}$$

Case 5. AC Bus-DC Line–Boost-DC Bus

This is the same version of Case 4 except that AC to DC bus connection is made through a DC/DC boost converter. This case is illustrated in Figure 21 and active power flow is calculated as

$$P_{nm}^{DC} = M_{nm}^{-1} V_n g_{nm} \left(M_{nm}^{-1} V_n - (1 - D_{mn}) V_m\right) \tag{53}$$

AC side power flow equations are

$$\begin{aligned} P_{nm} &= g_{nm} \left(M_{nm}^{-2} V_n^2 - (M_{nm}^{-1}(1 - D_{mn}) V_n V_m)\left(\frac{k_1}{\eta} + k_2 \eta\right)\right. \\ Q_{nm} &= P_{nm} tan\varphi_{VSC} \end{aligned} \tag{54}$$

where

$$\begin{aligned} &k_1 = 1, \quad k_2 = 0 \quad \text{if} \quad M_{nm}^{-1} V_n > (1 - D_{mn}) V_m \\ &k_1 = 0, \quad k_2 = 1 \quad \text{if} \quad M_{nm}^{-1} V_n < (1 - D_{mn}) V_m \\ &k_1 = 0.5, \quad k_2 = 0.5 \quad \text{if} \quad M_{nm}^{-1} V_n = (1 - D_{mn}) V_m \end{aligned} \tag{55}$$

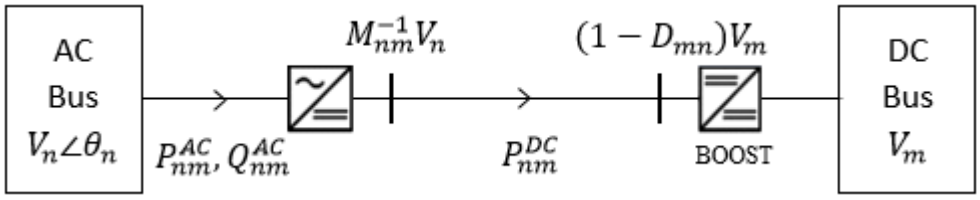

Figure 21. A Representative Schema for Case 5

Derivatives of line flow equations for Case 5 are

$$\begin{aligned}
\frac{dP_{nm}}{dV_n} &= g_{nm}\,(M_{nm}^{-2} * 2V_n - M_{nm}^{-1}(1 - D_{mn})V_m)(\frac{k_1}{\eta} + k_2\eta) \\
\frac{dQ_{nm}}{dV_n} &= tan\varphi_{VSC} * \frac{dP_{nm}}{dV_n} \\
\frac{dP_{nm}}{dV_m} &= g_{nm}\,(-M_{nm}^{-1}(1 - D_{mn})V_n)\left(\frac{k_1}{\eta} + k_2\eta\right) \\
\frac{dQ_{nm}}{dV_m} &= tan\varphi_{VSC} * \frac{dP_{nm}}{dV_m} \\
\frac{dP_{nm}}{dM_{nm}} &= g_{nm}\,(-2M_{nm}^{-3}V_n^2 + M_{nm}^{-2}(1 - D_{mn})V_nV_m)\left(\frac{k_1}{\eta} + k_2\eta\right) \\
\frac{dQ_{nm}}{dM_{nm}} &= tan\varphi_{VSC} * \frac{dP_{nm}}{dM_{nm}} \\
\frac{dP_{nm}}{dD_{mn}} &= g_{nm}\,(M_{nm}^{-1}V_nV_m)\left(\frac{k_1}{\eta} + k_2\eta\right)
\end{aligned} \tag{56}$$

Case 6. AC Bus-DC Line–Buck/Boost-DC Bus

In this case, AC and DC bus connection is made with a DC/DC buck-boost converter. System is illustrated in Figure 22. Active power flow on the line is expressed as

$$P_{nm}^{DC} = M_{nm}^{-1}V_n g_{nm}\,(M_{nm}^{-1}V_n - D_{mn}^{-1}(1 - D_{mn})V_m) \tag{57}$$

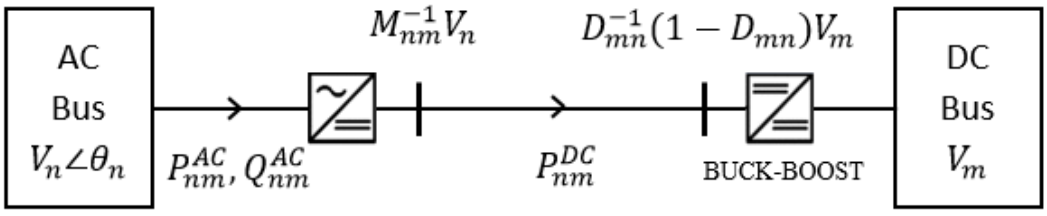

Figure 22. A Representative Schema for Case 6

AC side power flow equations are

$$P_{nm} = g_{nm}\,(M_{nm}^{-2}V_n^2 - (M_{nm}^{-1}D_{mn}^{-1}(1-D_{mn})V_nV_m)(\frac{k_1}{\eta}+k_2\eta)$$
$$Q_{nm} = P_{nm}tan\varphi_{VSC} \quad (58)$$

where

$$k_1 = 1, \quad k_2 = 0 \quad \text{if} \quad M_{nm}^{-1}V_n > D_{mn}^{-1}(1-D_{mn})V_m$$
$$k_1 = 0, \quad k_2 = 1 \quad \text{if} \quad M_{nm}^{-1}V_n < D_{mn}^{-1}(1-D_{mn})V_m \quad (59)$$
$$k_1 = 0.5, \quad k_2 = 0.5 \quad \text{if} \quad M_{nm}^{-1}V_n = D_{mn}^{-1}(1-D_{mn})V_m$$

Derivatives of line flow equations for Case 6 are

$$\frac{dP_{nm}}{dV_n} = g_{nm}\,(M_{nm}^{-2} * 2V_n - M_{nm}^{-1}D_{mn}^{-1}(1-D_{mn})V_m)(\frac{k_1}{\eta}+k_2\eta)$$
$$\frac{dQ_{nm}}{dV_n} = tan\varphi_{VSC} * \frac{dP_{nm}}{dV_n}$$
$$\frac{dP_{nm}}{dV_m} = g_{nm}\,(-M_{nm}^{-1}D_{mn}^{-1}(1-D_{mn})V_n)\left(\frac{k_1}{\eta}+k_2\eta\right)$$
$$\frac{dQ_{nm}}{dV_m} = tan\varphi_{VSC} * \frac{dP_{nm}}{dV_m} \quad (60)$$
$$\frac{dP_{nm}}{dM_{nm}} = g_{nm}\,(-2M_{nm}^{-3}V_n^2 + M_{nm}^{-2}D_{mn}^{-1}(1-D_{mn})V_nV_m)\left(\frac{k_1}{\eta}+k_2\eta\right)$$
$$\frac{dQ_{nm}}{dM_{nm}} = tan\varphi_{VSC} * \frac{dP_{nm}}{dM_{nm}}$$
$$\frac{dP_{nm}}{dD_{mn}} = g_{nm}\,(M_{nm}^{-1}D_{mn}^{-2}V_nV_m)\left(\frac{k_1}{\eta}+k_2\eta\right)$$

Case 7. DC Bus-DC Line-AC Bus

In this configuration, a DC line connects a DC bus to an AC bus and voltage conversion is performed with a VSC connected at the AC bus as shown in Figure 23. Active power flow can be expressed as

$$P_{nm}^{DC} = V_n g_{nm} (V_n - M_{mn}^{-1} V_m) = g_{nm}(V_n^2 - M_{mn}^{-1} V_n V_m) \tag{61}$$

Here, since there is no converter connected at the DC bus, efficiency constant is not present in the equation. Note that because equations are written from the DC side, there is no reactive power equation and derivatives of line flow equations for Case 7 are as follows

$$\begin{aligned} \frac{dP_{nm}}{dV_n} &= g_{nm} (2V_n - M_{mn}^{-1} V_m) \\ \frac{dP_{nm}}{dV_m} &= g_{nm} (- M_{mn}^{-1} V_n) \\ \frac{dP_{nm}}{dM_{mn}} &= g_{nm} (M_{mn}^{-2} V_n V_m) \end{aligned} \tag{62}$$

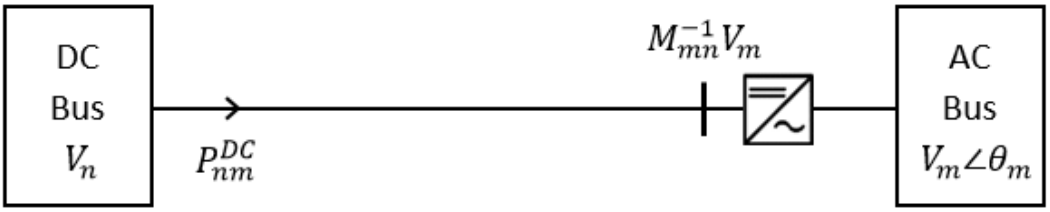

Figure 23. A Representative Schema for Case 7

Case 8. DC Bus-Buck-DC Line-AC Bus

In this case, a DC bus has a connection to an AC bus with a DC line through a DC/DC buck converter as illustrated in Figure 24. Active power flow can be expressed as

$$P_{nm} = g_{nm}(V_n^2 D_{nm}^{-2} - M_{mn}^{-1} D_{nm}^{-1} V_n V_m)\,(\frac{k_1}{\eta} + k_2\eta) \tag{63}$$

where

$$\begin{aligned} &k_1 = 1, \quad k_2 = 0 \quad \text{if} \quad D_{nm}^{-1} V_n > M_{mn}^{-1} V_m \\ &k_1 = 0, \quad k_2 = 1 \quad \text{if} \quad D_{nm}^{-1} V_n < M_{mn}^{-1} V_m \\ &k_1 = 0.5, \quad k_2 = 0.5 \quad \text{if} \quad D_{nm}^{-1} V_n = M_{mn}^{-1} V_m \end{aligned} \tag{64}$$

Derivatives of line flow equations for Case 8 are as follows

$$\begin{aligned} \frac{dP_{nm}}{dV_n} &= g_{nm}(2V_n D_{nm}^{-2} - M_{mn}^{-1} D_{nm}^{-1} V_m)\left(\frac{k_1}{\eta} + k_2\eta\right) \\ \frac{dP_{nm}}{dV_m} &= g_{nm}(-M_{mn}^{-1} D_{nm}^{-1} V_n)\left(\frac{k_1}{\eta} + k_2\eta\right) \\ \frac{dP_{nm}}{dM_{mn}} &= g_{nm}\,(\,M_{mn}^{-2} D_{nm}^{-1} V_n V_m)\left(\frac{k_1}{\eta} + k_2\eta\right) \\ \frac{dP_{nm}}{dD_{nm}} &= g_{nm}\,(\,-2D_{nm}^{-3} V_n^2 + M_{mn}^{-1} D_{nm}^{-2} V_n V_m)\left(\frac{k_1}{\eta} + k_2\eta\right) \end{aligned} \tag{65}$$

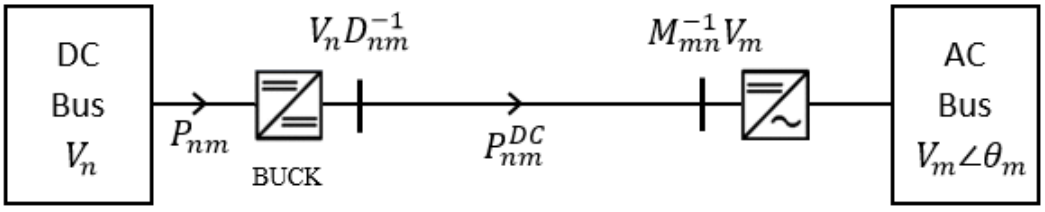

Figure 24. A Representative Schema for Case 8

Case 9. DC Bus-Boost-DC Line-AC Bus

In this configuration, a DC bus has a connection to an AC bus through a DC/DC boost converter as given in Figure 25. Active power flow can be expressed as

$$P_{nm} = g_{nm}(V_n^2(1-D_{nm})^2 - M_{mn}^{-1}(1-D_{nm})V_nV_m)\,(\frac{k_1}{\eta} + k_2\eta) \tag{66}$$

where

$$\begin{aligned} &k_1 = 1, \quad k_2 = 0 \quad \text{if} \quad (1-D_{nm})V_n > M_{mn}^{-1}V_m \\ &k_1 = 0, \quad k_2 = 1 \quad \text{if} \quad (1-D_{nm})V_n < M_{mn}^{-1}V_m \\ &k_1 = 0.5, \quad k_2 = 0.5 \quad \text{if} \quad (1-D_{nm})V_n = M_{mn}^{-1}V_m \end{aligned} \tag{67}$$

Derivatives of line flow equations for Case 9 are

$$\begin{aligned} \frac{dP_{nm}}{dV_n} &= g_{nm}(2V_n(1-D_{nm})^2 - M_{mn}^{-1}(1-D_{nm})V_m)\,(\frac{k_1}{\eta} + k_2\eta) \\ \frac{dP_{nm}}{dV_m} &= g_{nm}(-M_{mn}^{-1}(1-D_{nm})V_n)\left(\frac{k_1}{\eta} + k_2\eta\right) \\ \frac{dP_{nm}}{dM_{mn}} &= g_{nm}\,(\,M_{mn}^{-2}(1-D_{nm})V_nV_m)\left(\frac{k_1}{\eta} + k_2\eta\right) \\ \frac{dP_{nm}}{dD_{nm}} &= g_{nm}\,(-2(1-D_{nm})V_n^2 + M_{mn}^{-1}V_nV_m)\left(\frac{k_1}{\eta} + k_2\eta\right) \end{aligned} \tag{68}$$

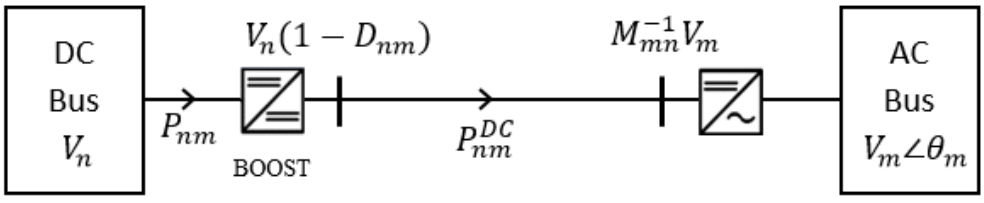

Figure 25. A Representative Schema for Case 9

Case 10. DC Bus-Buck-Boost-DC Line-AC Bus

In this case, a DC bus has a connection to an AC bus through a DC/DC buck-boost converter as given in Figure 26. Active power flow can be calculated as

$$P_{nm} = g_{nm}\left(\frac{V_n^2(1-D_{nm})^2}{D_{nm}^2} - \frac{(1-D_{nm})V_nV_m}{D_{nm}M_{mn}}\right)\left(\frac{k_1}{\eta} + k_2\eta\right) \tag{69}$$

where

$$\begin{aligned} &k_1 = 1, \quad k_2 = 0 \quad \text{if} \quad D_{nm}^{-1}(1-D_{nm})V_n > M_{mn}^{-1}V_m \\ &k_1 = 0, \quad k_2 = 1 \quad \text{if} \quad D_{nm}^{-1}(1-D_{nm})V_n < M_{mn}^{-1}V_m \\ &k_1 = 0.5, \quad k_2 = 0.5 \quad \text{if} \quad D_{nm}^{-1}(1-D_{nm})V_n = M_{mn}^{-1}V_m \end{aligned} \tag{70}$$

Derivatives of line flow equations for Case 10 are

$$\begin{aligned} \frac{dP_{nm}}{dV_n} &= g_{nm}\left(\frac{2V_n(1-D_{nm})^2}{D_{nm}^2} - \frac{(1-D_{nm})V_m}{D_{nm}M_{mn}}\right)\left(\frac{k_1}{\eta} + k_2\eta\right) \\ \frac{dP_{nm}}{dV_m} &= g_{nm}\left(-\frac{(1-D_{nm})V_n}{D_{nm}M_{mn}}\right)\left(\frac{k_1}{\eta} + k_2\eta\right) \\ \frac{dP_{nm}}{dM_{mn}} &= g_{nm}\left(\frac{(1-D_{nm})V_nV_m}{D_{nm}M_{mn}^2}\right)\left(\frac{k_1}{\eta} + k_2\eta\right) \\ \frac{dP_{nm}}{dD_{nm}} &= g_{nm}\left[-2V_n^2\left(\frac{(1-D_{nm})}{D_{nm}^2} + \frac{(1-D_{nm})^2}{D_{nm}^3}\right) + \frac{V_nV_m}{M_{mn}}\left(\frac{1}{D_{nm}}\right.\right. \\ &\qquad \left.\left. + \frac{(1-D_{nm})}{D_{nm}^2}\right)\right]\left(\frac{k_1}{\eta} + k_2\eta\right) \end{aligned} \tag{71}$$

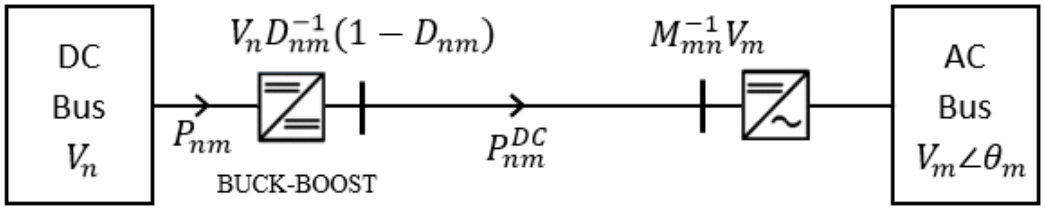

Figure 26. A Representative Schema for Case 10

Case 11. DC Bus-DC Line-DC Bus

Two DC buses are connected together with a DC line as illustrated in Figure 27. Active power flow can be expressed as

$$P_{nm} = g_{nm}(V_n^2 - V_n V_m) \tag{72}$$

Derivatives of line flow equations for Case 11 are

$$\begin{aligned} \frac{dP_{nm}}{dV_n} &= g_{nm}(2V_n - V_m) \\ \frac{dP_{nm}}{dV_m} &= g_{nm}(-V_n) \end{aligned} \tag{73}$$

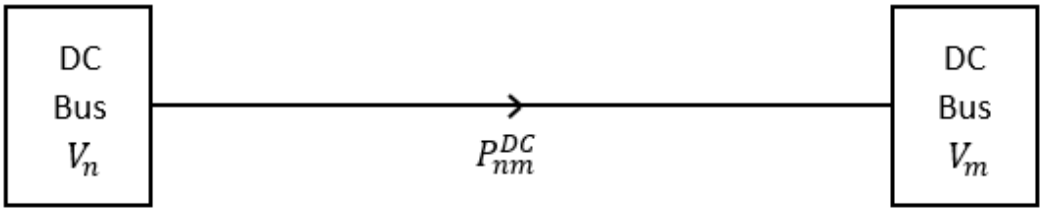

Figure 27. A Representative Schema for Case 11

Case 12. DC Bus-Buck-DC Line-DC Bus

Figure 28 shows connection of two DC buses with a DC/DC buck converter. Active power flow can be expressed as

$$P_{nm} = g_{nm}(V_n^2 D_{nm}^{-2} - D_{nm}^{-1} V_n V_m)\,(\frac{k_1}{\eta} + k_2 \eta) \tag{74}$$

where

$$\begin{aligned} &k_1 = 1, \quad k_2 = 0 \quad \text{if} \quad D_{nm}^{-1} V_n > V_m \\ &k_1 = 0, \quad k_2 = 1 \quad \text{if} \quad D_{nm}^{-1} V_n < V_m \\ &k_1 = 0.5, \quad k_2 = 0.5 \quad \text{if} \quad D_{nm}^{-1} V_n = V_m \end{aligned} \tag{75}$$

Derivatives of line flow equations for Case 12 are

$$\begin{aligned} \frac{dP_{nm}}{dV_n} &= g_{nm}(2V_n D_{nm}^{-2} - D_{nm}^{-1} V_m)(\frac{k_1}{\eta} + k_2 \eta) \\ \frac{dP_{nm}}{dV_m} &= g_{nm}(-D_{nm}^{-1} V_n)(\frac{k_1}{\eta} + k_2 \eta) \\ \frac{dP_{nm}}{dD_{nm}} &= g_{nm}(-2V_n^2 D_{nm}^{-3} + D_{nm}^{-2} V_n V_m)\,(\frac{k_1}{\eta} + k_2 \eta) \end{aligned} \tag{76}$$

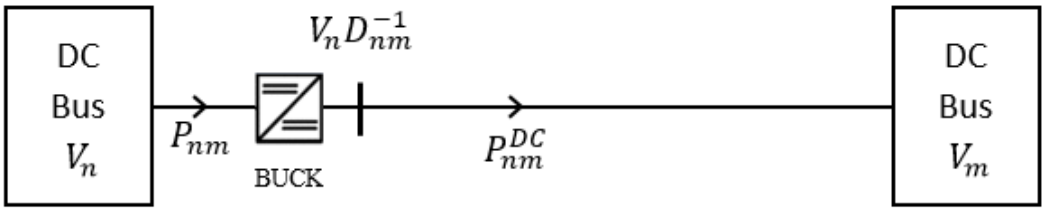

Figure 28. A Representative Schema for Case 12

Case 13. DC Bus-Boost-DC Line-DC Bus

Figure 29 shows connection of two DC buses with a DC/DC boost converter. Active power flow can be expressed as

$$P_{nm} = g_{nm}(V_n^2(1 - D_{nm})^2 - (1 - D_{nm})V_nV_m)\,(\frac{k_1}{\eta} + k_2\eta) \tag{77}$$

where

$$\begin{aligned} &k_1 = 1, \quad k_2 = 0 \quad \text{if} \quad (1 - D_{nm})V_n > V_m \\ &k_1 = 0, \quad k_2 = 1 \quad \text{if} \quad (1 - D_{nm})V_n < V_m \\ &k_1 = 0.5, \quad k_2 = 0.5 \quad \text{if} \quad (1 - D_{nm})V_n = V_m \end{aligned} \tag{78}$$

Derivatives of line flow equations for Case 13 are

$$\begin{aligned} \frac{dP_{nm}}{dV_n} &= g_{nm}(2V_n(1 - D_{nm})^2 - (1 - D_{nm})V_m)(\frac{k_1}{\eta} + k_2\eta) \\ \frac{dP_{nm}}{dV_m} &= g_{nm}(-(1 - D_{nm})V_n)(\frac{k_1}{\eta} + k_2\eta) \\ \frac{dP_{nm}}{dD_{nm}} &= g_{nm}(-2V_n^2(1 - D_{nm}) + V_nV_m)\,(\frac{k_1}{\eta} + k_2\eta) \end{aligned} \tag{79}$$

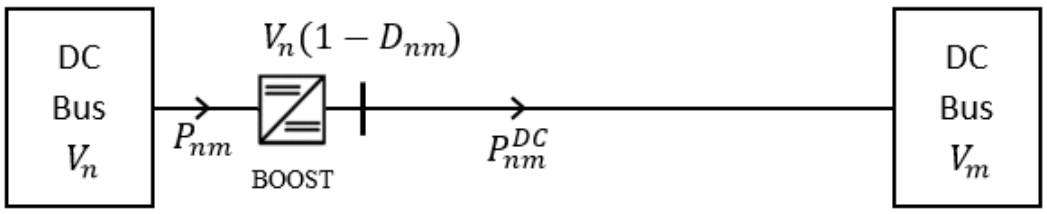

Figure 29. A Representative Schema for Case 13

Case 14. DC Bus-Buck-Boost-DC Line-DC Bus

As Figure 30 shows, two DC buses are connected with a DC/DC buck-boost converter. Active power flowing from DC bus n can be written as

$$P_{nm} = g_{nm}(V_n^2 D_{nm}^{-2}(1 - D_{nm})^2 - D_{nm}^{-1}(1 - D_{nm})V_n V_m)\ (\frac{k_1}{\eta} + k_2\eta) \tag{80}$$

where

$$\begin{aligned} &k_1 = 1, \quad k_2 = 0 \quad \text{if} \quad D_{nm}^{-1}(1 - D_{nm})V_n > V_m \\ &k_1 = 0, \quad k_2 = 1 \quad \text{if} \quad D_{nm}^{-1}(1 - D_{nm})V_n < V_m \\ &k_1 = 0.5, \quad k_2 = 0.5 \quad \text{if} \quad D_{nm}^{-1}(1 - D_{nm})V_n = V_m \end{aligned} \tag{81}$$

Derivatives of line flow equations for Case 14 are

$$\begin{aligned} \frac{dP_{nm}}{dV_n} &= g_{nm}(2V_n D_{nm}^{-2}(1 - D_{nm})^2 - D_{nm}^{-1}(1 - D_{nm})V_m)(\frac{k_1}{\eta} + k_2\eta) \\ \frac{dP_{nm}}{dV_m} &= g_{nm}(-D_{nm}^{-1}(1 - D_{nm})V_n)(\frac{k_1}{\eta} + k_2\eta) \\ \frac{dP_{nm}}{dD_{nm}} &= g_{nm}[-2V_n^2(D_{nm}^{-2}(1 - D_{nm}) + D_{nm}^{-3}(1 - D_{nm})^2) \\ &\quad + V_n V_m D_{nm}^{-2}](\frac{k_1}{\eta} + k_2\eta) \end{aligned} \tag{82}$$

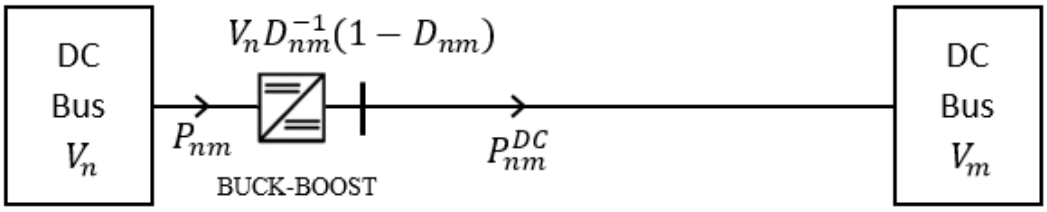

Figure 30. A Representative Schema for Case 14

Case 15. DC Bus- DC Line-Buck-DC Bus

Figure 31 illustrates the connection of two DC buses with a DC/DC buck converter and a DC line. Active power flow can be expressed as

$$P_{nm} = g_{nm}(V_n^2 - D_{mn}^{-1}V_nV_m) \tag{83}$$

Derivatives of line flow equations for Case 15 are

$$\begin{aligned}
\frac{dP_{nm}}{dV_n} &= g_{nm}(2V_n - D_{mn}^{-1}V_m) \\
\frac{dP_{nm}}{dV_m} &= g_{nm}(-D_{mn}^{-1}V_n) \\
\frac{dP_{nm}}{dD_{mn}} &= g_{nm}(D_{mn}^{-2}V_nV_m)
\end{aligned} \tag{84}$$

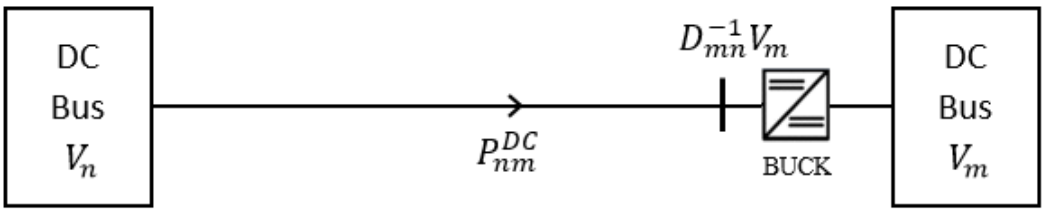

Figure 31. A Representative Schema for Case 15

Case 16. DC Bus- DC Line-Boost-DC Bus

Connection of two DC buses with a DC/DC boost converter is given Figure 32. Active power flow can be expressed as

$$P_{nm} = g_{nm}(V_n^2 - (1 - D_{mn})V_n V_m) \tag{85}$$

Derivatives of line flow equations for Case 16 are

$$\begin{aligned} \frac{dP_{nm}}{dV_n} &= g_{nm}(2V_n - (1 - D_{mn})V_m) \\ \frac{dP_{nm}}{dV_m} &= g_{nm}(-(1 - D_{mn})V_n) \\ \frac{dP_{nm}}{dD_{mn}} &= g_{nm}(V_n V_m) \end{aligned} \tag{86}$$

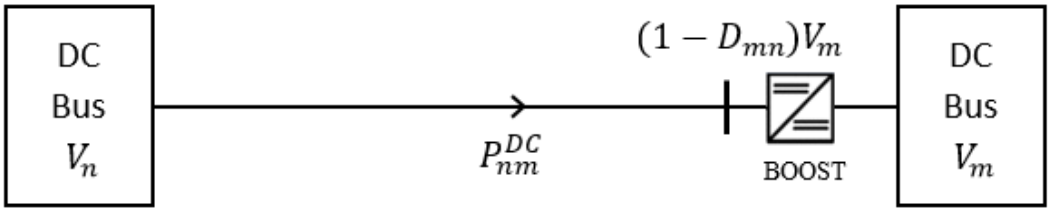

Figure 32. A Representative Schema for Case 16

Case 17. DC Bus- DC Line-Buck-Boost-DC Bus

Connection of two DC buses with a DC/DC buck-boost converter is illustrated in Figure 33. Active power flow can be expressed as

$$P_{nm} = g_{nm}(V_n^2 - D_{mn}^{-1}(1 - D_{mn})V_nV_m) \tag{87}$$

Derivatives of line flow equations for Case 17 are

$$\begin{aligned}
\frac{dP_{nm}}{dV_n} &= g_{nm}(2V_n - D_{mn}^{-1}(1 - D_{mn})V_m) \\
\frac{dP_{nm}}{dV_m} &= g_{nm}(-D_{mn}^{-1}(1 - D_{mn})V_n) \\
\frac{dP_{nm}}{dD_{mn}} &= g_{nm}(D_{mn}^{-2}V_nV_m)
\end{aligned} \tag{88}$$

This concludes all partial derivatives which are required when obtaining the Jacobian matrix. One can easily construct required Jacobian matrix by properly utilizing given equations.

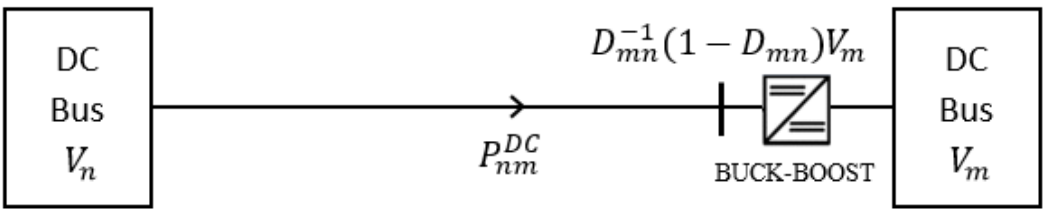

Figure 33. A Representative Schema for Case 17

CHAPTER 4

IMPLEMENTATION IN VARIOUS TEST SYSTEMS

Proposed load flow algorithm is implemented in MATLAB. Number of buses, bus types, specified voltage magnitudes, generator and load data, line types, line impedances and converter types are all provided in a separate "txt" file and MATLAB reads necessary data from it. In this chapter, load flow algorithm is implemented in various test systems and results are presented together with the results produced by PSCAD/EMTDC software, and generalized reduced gradient (GRG) method. Proposed load flow algorithm is executed on a computer with Intel Core i5 M480 2.67GHz CPU, 6 GB RAM, 64 bit.

4.1 Test System I

First of all, proposed load flow calculation method is utilized in a sample AC/DC distribution system which has 13 buses and four VSCs as Figure 34 illustrates [1]. VSC converters are implemented for AC to DC conversion and load data information is provided for each bus. First bus is chosen as a slack bus (or reference bus) and it has "1.05 p.u." voltage magnitude and "0 degrees" phase angle. DC lines are also incorporated with AC lines and line flows are calculated. VSCs have different modulation indexes and the efficiency (η) of all converters are 98%.

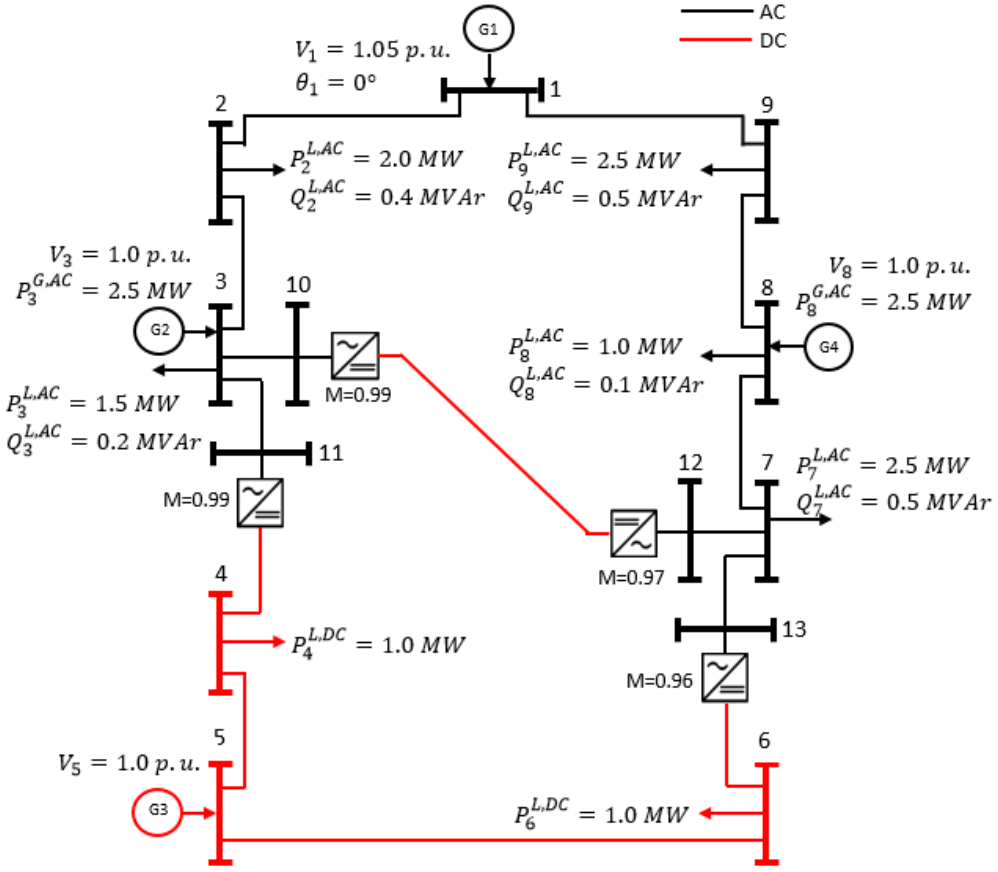

Figure 34. Representation of Test System I

Base value for the complex power is 10 MVA, DC base voltage is 6.8 kV and AC base voltage is 4.16 kV. Power factor is 95% for all converters and all VSCs are operating in constant modulation index mode. Bus types are given in Table 5 and generators active power ratings and reactive power limits are provided in Table 6.

Table 5. Bus types of Test System I

Bus Type	Bus Number
AC Slack Bus	1
AC PV Bus	3, 8
AC PQ Bus	2, 7, 9, 10, 11, 12, 13
Vdc Bus	5
Pdc Bus	4, 6

Table 6. Generator Limits of Test System I

	P Limit		Q Limit	
Generator	Pmax (MW)	Pmin (MW)	Qmax (MVAr)	Qmin (MVAr)
G2	-	-	0.75	0.1
G3	2	0.5	-	-
G4	-	-	0.75	0.1

AC and DC line impedances are provided in Table 7. Note that DC lines only have DC line resistances. The load flow algorithm is executed 10 times in MATLAB on a computer with i5 2.67 GHz processor, 6 GB RAM and average execution time is found as 24.5 ms, whereas reduced gradient algorithm execution time in [1] is stated as 124 ms on a computer with i7 3.4GHz processor, 8 GB RAM.

Table 7. Line Impedances of Test System I

Between Buses	G+jB (Ω)
1-2	0.2218+j0.363
1-9	0.2218+j0.363
2-3	0.887+j1.4520
3-10	0.05+j0.754
3-11	0.05+j0.754
4-5	0.2208
4-11	0.4415
5-6	0.2208
6-13	0.4415
7-8	0.4435+j0.726
7-12	0.05+j0.754
7-13	0.05+j0.754
8-9	0.4435+j0.726
10-12	0.883

Algorithm convergence criteria is set such that the maximum absolute value of mismatch should be less than 10^{-10} p.u. and after four iterations algorithm has converged and no generator limits are violated. Analysis results and generation data are provided in Table 8 and Table 9 respectively in comparison with other approaches. Results indicate that all three methods converge almost to same results and they are consistent with each other.

Table 8. Load Flow Results of Test System I

Bus	Proposed		PSCAD [1]		Reduced Gradient [1]	
	Voltage (p.u.)	Phase θ (degrees)	Voltage (p.u.)	Phase θ (degrees)	Voltage (p.u.)	Phase θ (degrees)
1	1.050	0.000	1.050	0.000	1.050	0.000
2	1.013	-2.072	1.013	-2.077	1.013	-2.063
3	1.000	-2.436	1.000	-2.464	1.000	-2.464
4	0.997	-	0.997	-	0.997	-
5	1.000	-	1.000	-	1.000	-
6	0.994	-	0.994	-	0.994	-
7	0.946	-6.643	0.946	-6.640	0.946	-6.646
8	1.000	-2.984	1.000	-2.979	1.000	-2.979
9	1.004	-2.657	1.004	-2.656	1.004	-2.636
10	0.988	-4.054	0.988	-4.107	0.988	-4.068
11	0.992	-3.583	0.992	-3.627	0.992	-3.610
12	0.956	-4.966	0.956	-4.988	0.956	-4.985
13	0.951	-5.808	0.951	-5.840	0.951	-5.787

Table 9. Generation Data of Test System I

Generator	Generation					
	Proposed		PSCAD [1]		Reduced Gradient [1]	
	Active Power P (MW)	Reactive Power Q (MVAr)	Active Power P (MW)	Reactive Power Q (MVAr)	Active Power P (MW)	Reactive Power Q (MVAr)
G1	4.9208	1.2398	4.9240	1.2390	4.9210	1.2399
G2	2.5000	0.5253	2.5000	0.5305	2.5000	0.5300
G3	1.8704	-	1.8726	-	1.8701	-
G4	2.5000	0.4241	2.5000	0.4266	2.5000	0.4238

Maximum deviation of the voltage magnitude from the PSCAD result for the presented methodology can be calculated as

$$\%\ Max\ Deviation = max\left|\frac{Implemented - PSCAD\ Result}{PSCAD\ Result}\right| x100 \qquad (89)$$

and it is just 0.04% which is the same for the reduced gradient method. Voltage phase angle maximum deviation is 0.94% for the reduced gradient method and 1.29% for the proposed algorithm. Power flows are given in Table 10 and the total system loss including line and converter losses is found as 0.291 MW + 0.489 MVAr.

Table 10. Power Flows of Test System I

Sending	Receiving	Proposed		PSCAD [1]		Reduced Gradient [1]	
		Active Power P (MW)	Reactive Power Q (MVAr)	Active Power P (MW)	Reactive Power Q (MVAr)	Active Power P (MW)	Reactive Power Q (MVAr)
1	2	2.1826	0.5734	2.1860	0.5716	2.1830	0.5733
2	1	-2.1234	-0.4765	-2.1270	-0.4744	-2.1238	-0.4764
1	9	2.7382	0.6664	2.7370	0.6670	2.7380	0.6666
9	1	-2.6458	-0.5153	-2.6450	-0.5160	-2.6457	-0.5156
2	3	0.1234	0.0765	0.1269	0.0744	0.1238	0.0764
3	2	-0.1224	-0.0748	-0.1258	-0.0727	-0.1227	-0.0746
3	10	0.6561	0.2364	0.6572	0.2380	0.6564	0.2365
10	3	-0.6547	-0.2152	-0.6520	-0.2120	-0.6550	-0.2153
3	11	0.4663	0.1637	0.4676	0.1651	0.4663	0.1637
11	3	-0.4656	-0.1530	-0.4630	-0.1503	-0.4656	-0.1530
4	5	-0.5457	-	-0.5479	-	-0.5457	-
5	4	0.5471	-	0.5493	-	0.5471	-
4	11	-0.4543	-	-0.4521	-	-0.4543	-
11	4	0.4562	-	0.4541	-	0.4563	-
5	6	1.3233	-	1.3233	-	1.3230	-
6	5	-1.3149	-	-1.3149	-	-1.3147	-
6	13	0.3149	-	0.3149	-	0.3147	-
13	6	-0.3139	-	-0.3140	-	-0.3137	-
7	8	-1.5730	-0.2202	-1.5750	-0.2230	-1.5729	-0.2201
8	7	1.6453	0.3385	1.6470	0.3417	1.6452	0.3385
7	12	-0.6196	-0.1838	-0.6192	-0.1826	-0.6200	-0.1838
12	7	0.6210	0.2041	0.6236	0.2075	0.6213	0.2042
7	13	-0.3074	-0.0961	-0.3061	-0.0944	-0.3071	-0.0960
13	7	0.3077	0.1011	0.3106	0.1040	0.3074	0.1011
8	9	-0.1453	-0.0144	-0.1443	-0.0151	-0.1452	-0.0147
9	8	0.1458	0.0153	0.1449	0.0160	0.1457	0.0156
10	12	0.6416	-	0.6420	-	0.6419	-
12	10	-0.6336	-	-0.6341	-	-0.6340	-

Now, to evaluate the algorithm performance in all aspects, operating modes of the VSCs connected at bus 13 and bus 10 are changed from the constant modulation index mode to the constant voltage mode. Voltage magnitude of bus 13 is held at 0.951 p.u. and voltage magnitude of bus 10 is held at 0.988 p.u. by VSCs to be consistent with the previous system. This modified distribution system is illustrated in Figure 35. Two new unknowns M_{10-12} and M_{13-6} are introduced and they are initialized as "1.0" at the beginning.

After applying the proposed algorithm, it has successfully converged to a solution in four iterations. Average time of 10 executions found to be 31.5 ms and unknown VSC modulation indexes together with unknown bus voltages are calculated as given in Table 11.

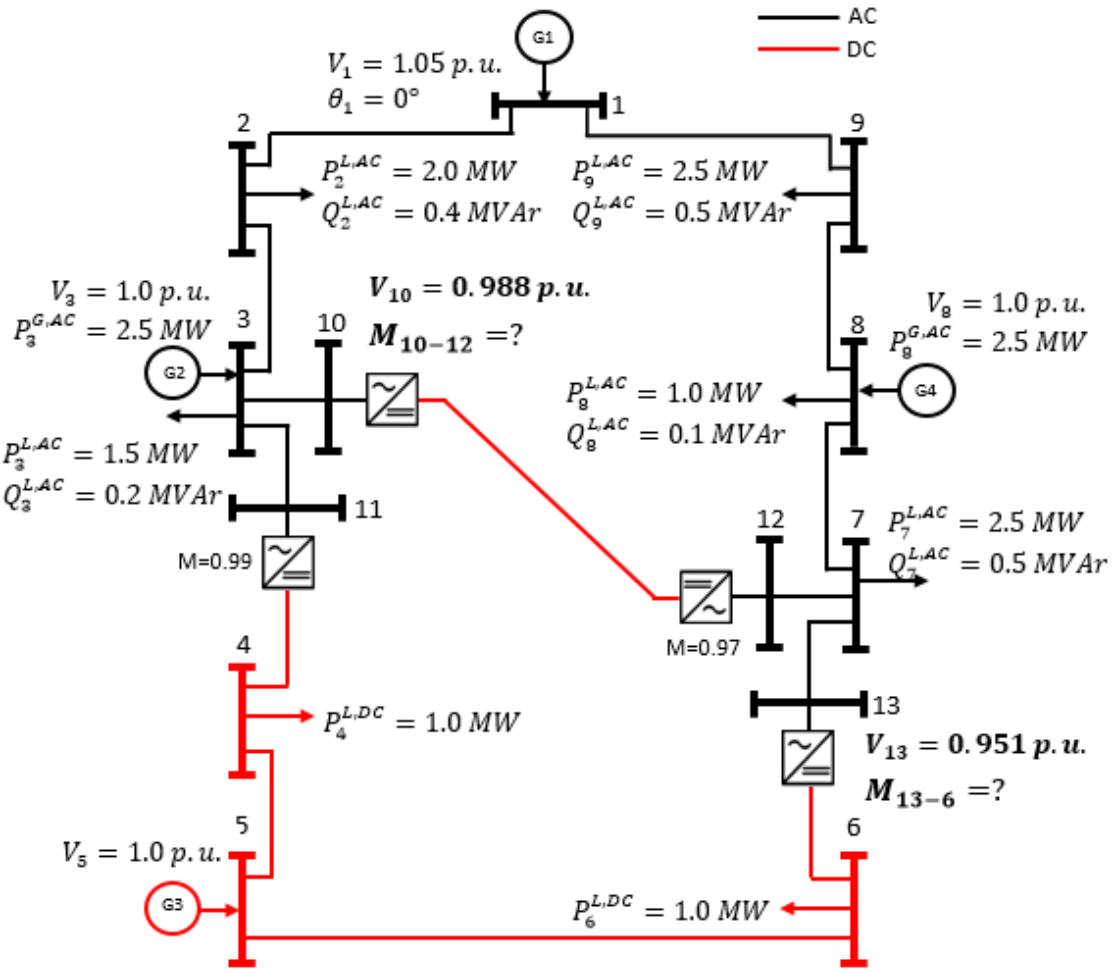

Figure 35. Representation of Modified Test System I

Table 11. Results of Modified Test System I

Bus	Voltage (p.u.)	Phase θ (degrees)	Bus	Voltage (p.u.)	Phase θ (degrees)
1	1.050	0.000	9	1.004	-2.653
2	1.013	-2.088	10	0.988	-4.167
3	1.000	-2.523	11	0.992	-3.669
4	0.997	-	12	0.957	-4.920
5	1.000	-	13	0.951	-5.808
6	0.994	-	Other Unknowns		
7	0.946	-6.624	$M_{10-12} = 0.9893$		
8	1.000	-2.970	$M_{13-6} = 0.9599$		

Results show the consistency of the method that modulation indexes are very close to the previous case, where VSCs are operating in the constant modulation index mode, to be able to sustain the same voltage magnitudes with the first case on bus 10 and bus 13. Modulation index difference from the previous case is 0.0007 for M_{10-12} and 0.0001 for M_{13-6}.

4.2 Test System II

This sample distribution system includes 33 buses with various loads and converters as illustrated in Figure 36 [1]. Proposed load flow analysis method is performed on this 33-bus system with seven VSCs operating in constant modulation index mode and many AC/DC converters connected to various loads. Load power demands are given in Table 12 and line impedances are provided in Table 13. DC base voltage is 20.67 kV and AC base voltage is 12.66 kV. Base power is taken as 10 MVA, power factor for VSCs and the efficiency (η) of all converters are 95%.

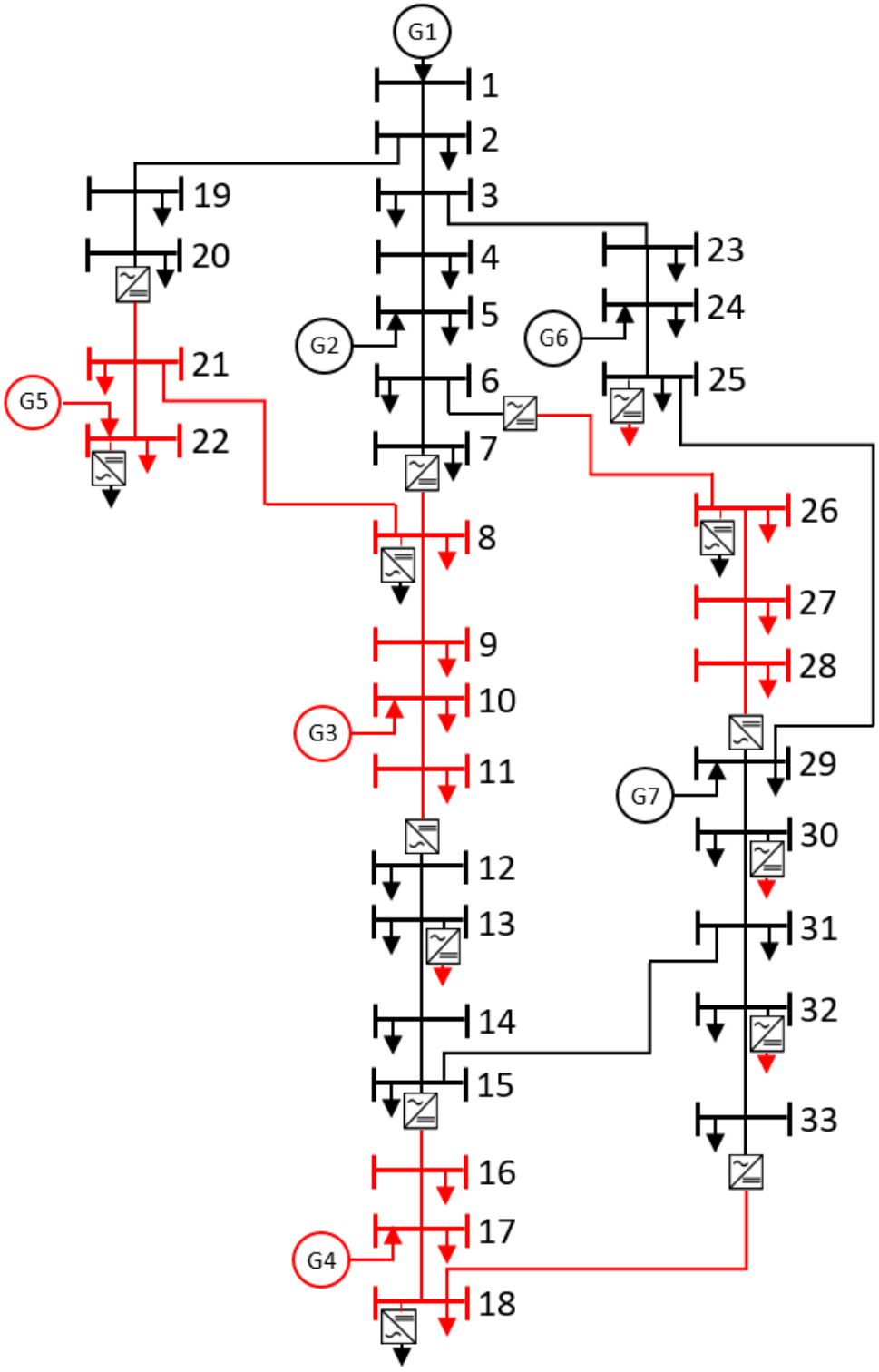

Figure 36. Representation of Test System II

Table 12. Load Power Demands of Test System II

	AC Load		DC Load		AC Load		DC Load
Load @ Bus	$P^{L,AC}$ (kW)	$Q^{L,AC}$ (kVAr)	$P^{L,DC}$ (kW)	Load @ Bus	$P^{L,AC}$ (kW)	$Q^{L,AC}$ (kVAr)	$P^{L,DC}$ (kW)
1	-	-	-	18	45	20	45
2	200	120	-	19	180	80	-
3	180	80	-	20	180	80	-
4	240	160	-	21	-	-	300
5	125	60	-	22	90	45	90
6	200	100	-	23	180	100	-
7	200	100	-	24	115	60	-
8	120	70	120	25	300	100	300
9	-	-	120	26	60	35	60
10	-	-	120	27	-	-	200
11	-	-	300	28	-	-	120
12	120	70	-	29	85	35	-
13	60	15	60	30	100	60	100
14	400	200	-	31	170	50	-
15	260	105	-	32	145	70	145
16	-	-	60	33	240	160	-
17	-	-	60				

Table 13. Line Impedances of Test System II

Between Buses	G+jB (Ω)	Between Buses	G+jB (Ω)
1-2	0.0922+j0.0470	15-31	2.0000+j2.0000
2-3	0.4930+j0.2511	16-17	2.5780
2-19	0.1640+j0.1565	16-22	4.0000
3-4	0.3660+j0.1864	17-18	1.4640
3-23	0.4512+j0.3083	18-33	1.0000
4-5	0.3811+j0.1941	19-20	1.5042+j1.3554
5-6	0.819+j0.7070	20-21	0.8190
6-7	0.1872+j0.6188	21-22	1.4178
6-26	0.4060	23-24	0.8980+j0.7091
7-8	1.4228	24-25	0.8960+j0.7011
8-9	2.0600	25-29	0.5+j0.5
8-21	4.0000	26-27	0.5684
9-10	2.0880	27-28	2.1180
10-11	0.3932	28-29	1.6084
11-12	0.7488	29-30	0.5075+j0.2585
12-13	1.4680	30-31	0.9744+j0.9630
13-14	0.5416	31-32	0.3105+j0.3619
14-15	0.5910	32-33	0.3410+j0.5302
15-16	1.4926		

First bus is assigned as a slack bus and "1.05 p.u." voltage magnitude and "0 degrees" phase angle are assigned. Voltage magnitudes of other generator buses are specified as $V_5 = 1.03\ p.u.$, $V_{24} = 1.03\ p.u.$, $V_{29} = 1.02\ p.u.$ and modulation indexes of all VSCs are listed in Table 14. Generator power ratings and limits are also provided in Table 15.

Table 14. VSC Modulation Indexes of Test System II

VSC @ Bus	Modulation Index
6	0.97
7	0.99
12	0.97
15	0.96
20	0.99
29	0.98
33	0.96

Table 15. Generator Ratings of Test System II

Generator	P (MW)	Qmax (MVAr)	Qmin (MVAr)
G2	0.5	0.25	0.05
G3	0.25	-	-
G4	0.25	-	-
G5	0.25	-	-
G6	0.5	0.25	0.05
G7	0.5	0.25	0.05

Newton-Raphson iterative method based algorithm is implemented in MATLAB and results of this method and reduced gradient approach are compared. Algorithm is converged with a maximum absolute value of mismatch being less than 10^{-10} after five iterations.

Analysis results and generation data are provided in Table 16 and Table 17. Voltage magnitude and phase angle discrepancy between the proposed approach and reduced gradient method is 0.01% maximum.

Table 16. Load Flow Analysis Results of Test System II

Bus	Proposed		Reduced Gradient [1]		Bus	Proposed		Reduced Gradient [1]	
	Voltage (p.u.)	Phase θ (degrees)	Voltage (p.u.)	Phase θ (degrees)		Voltage (p.u.)	Phase θ (degrees)	Voltage (p.u.)	Phase θ (degrees)
1	1.0500	0.0000	1.0500	0.0000	18	1.0393	-	1.0393	-
2	1.0471	-0.0097	1.0471	-0.0097	19	1.0450	-0.0593	1.0450	-0.0593
3	1.0378	-0.0278	1.0378	-0.0278	20	1.0287	-0.4395	1.0287	-0.4395
4	1.0336	-0.0368	1.0336	-0.0368	21	1.0370	-	1.0370	-
5	1.0300	-0.0511	1.0300	-0.0511	22	1.0371	-	1.0372	-
6	1.0191	-0.2769	1.0191	-0.2769	23	1.0348	-0.0534	1.0348	-0.0534
7	1.0187	-0.2989	1.0187	-0.2989	24	1.0300	-0.1185	1.0300	-0.1185
8	1.0292	-	1.0292	-	25	1.0224	-0.2187	1.0224	-0.2187
9	1.0267	-	1.0267	-	26	1.0495	-	1.0495	-
10	1.0248	-	1.0248	-	27	1.0481	-	1.0481	-
11	1.0243	-	1.0243	-	28	1.0437	-	1.0437	-
12	0.9932	-0.6232	0.9932	-0.6232	29	1.0200	-0.2249	1.0200	-0.2249
13	0.9921	-0.6657	0.9922	-0.6657	30	1.0140	-0.2491	1.0140	-0.2491
14	0.9922	-0.6636	0.9923	-0.6636	31	1.0023	-0.5056	1.0023	-0.5056
15	0.9945	-0.6294	0.9945	-0.6294	32	1.0001	-0.5722	1.0001	-0.5722
16	1.0369	-	1.0369	-	33	0.9982	-0.6348	0.9982	-0.6349
17	1.0388	-	1.0388	-					

Table 17. Generation Data of Test System II

Generator	Generation			
	Proposed		Reduced Gradient [1]	
	Active Power P (MW)	Reactive Power Q (MVAr)	Active Power P (MW)	Reactive Power Q (MVAr)
G1	4.3435	1.8900	4.3435	1.8900
G2	0.5000	0.1400	0.5000	0.1400
G3	0.2500	-	0.2500	-
G4	0.2500	-	0.2500	-
G5	0.2500	-	0.2500	-
G6	0.5000	0.2435	0.5000	0.2435
G7	0.5000	0.0819	0.5000	0.0819

Line flows are provided in Table 18 and total system loss including line and converter losses is calculated as 0.399 MW+0.380 MVAr. Reduced gradient algorithm execution time is stated as 207 ms on a computer with i7 3.4GHz processor, 8 GB RAM [1]. Proposed Newton-Raphson based algorithm is executed 10 times in Matlab on a computer with i5 2.67GHz processor, 6 GB RAM and average execution time is found as 44.2 ms.

Table 18. Power Flows of Test System II

Sending	Receiving	Newton-Raphson		Reduced Gradient [1]		Sending	Receiving	Newton-Raphson		Reduced Gradient [1]	
		Active Power P (MW)	Reactive Power Q (MVAr)	Active Power P (MW)	Reactive Power Q (MVAr)			Active Power P (MW)	Reactive Power Q (MVAr)	Active Power P (MW)	Reactive Power Q (MVAr)
1	2	4.3435	1.8900	4.3435	1.8900	15	31	-0.3967	-0.2241	-0.3967	-0.2241
2	3	2.5664	1.1956	2.5664	1.1956	31	15	0.3993	0.2267	0.3993	0.2267
2	19	1.5654	0.5684	1.5654	0.5684	16	17	-0.3294	-	-0.3294	-
3	4	1.5333	0.7069	1.5333	0.7069	16	22	-0.0254	-	-0.0254	-
3	23	0.8306	0.3973	0.8307	0.3973	22	16	0.0254	-	0.0254	-
4	5	1.2872	0.5438	1.2872	0.5438	17	18	-0.1400	-	-0.1400	-
5	6	1.6579	0.6216	1.6579	0.6216	18	33	-0.2325	-	-0.2325	-
6	7	0.1260	0.0757	0.1260	0.0757	33	18	0.2448	0.0805	0.2448	0.0805
6	26	1.3168	0.4328	1.3168	0.4328	19	20	1.3828	0.4859	1.3828	0.4859
26	6	-1.2496	-	-1.2496	-	20	21	1.1844	0.38928	1.1843	0.38928
7	8	-0.0741	-0.0243	-0.0741	-0.0243	21	20	-1.1229	-	-1.1229	-
8	7	0.0780	-	0.0780	-	21	22	-0.0398	-	-0.0398	-
8	9	0.5319	-	0.5319	-	23	24	0.6484	0.2958	0.6484	0.2958
8	21	-0.8562	-	-0.8562	-	24	25	1.0308	0.4772	1.0308	0.4772
21	8	0.8627	-	0.8627	-	25	29	0.4082	0.3719	0.4082	0.3719
9	10	0.4107	-	0.4107	-	26	27	1.1265	-	1.1265	-
10	11	0.5399	-	0.5399	-	27	28	0.9249	-	0.9250	-
11	12	0.2396	-	0.2396	-	28	29	0.8011	-	0.8011	-
12	11	-0.2275	-0.0748	-0.2275	-0.0748	29	28	-0.7589	-0.2494	-0.7589	-0.2495
12	13	0.1075	0.0048	0.1075	0.0048	29	30	1.5812	0.6673	1.5812	0.6673
13	14	-0.0157	-0.0103	-0.0157	-0.0103	30	31	1.3670	0.6027	1.3670	0.6028
14	15	-0.4157	-0.2103	-0.4157	-0.2103	31	32	0.7845	0.3130	0.7845	0.3130
15	16	-0.2798	-0.0920	-0.2798	-0.0920	32	33	0.4854	0.2414	0.4854	0.2414
16	15	0.2948	-	0.2948	-						

Now, operating modes of VSCs connected at bus 12, bus 15 and bus 33 are changed to constant voltage mode and they are assigned to maintain constant voltage magnitudes equal to ones found in the case for constant modulation index mode as $V_{12} = 0.9932\ p.u.$, $V_{15} = 0.9945\ p.u.$, $V_{33} = 0.9982\ p.u.$

Unknown modulation indexes M_{12-11}, M_{15-16} and M_{33-18} are initialized as "1.0" before starting to analysis as given in Table 19. Then, proposed algorithm is applied and it has successfully converged to a solution with a time average of 10 executions found to be 40 ms. Calculated unknown bus voltages and VSC modulation indexes are shown in Table 20.

Table 19. Assigned Modulation Indexes and Operating Modes of VSCs

VSC @ Bus	Modulation Index	Operating Mode	Bus Voltage
6	0.97	Constant M	to be calculated
7	0.99	Constant M	to be calculated
12	**1.00**	**Constant V**	0.9932 p.u.
15	**1.00**	**Constant V**	0.9945 p.u.
20	0.99	Constant M	to be calculated
29	0.98	Constant M	to be calculated
33	**1.00**	**Constant V**	0.9982 p.u.

Table 20. Load Flow Analysis Results of Modified Test System II

Bus	Voltage (p.u.)	Phase θ (degrees)	Bus	Voltage (p.u.)	Phase θ (degrees)
1	1.0500	0.0000	20	1.0287	-0.4393
2	1.0471	-0.0098	21	1.0370	-
3	1.0378	-0.0281	22	1.0372	-
4	1.0336	-0.0372	23	1.0348	-0.0540
5	1.0300	-0.0514	24	1.0300	-0.1199
6	1.0191	-0.2772	25	1.0224	-0.2206
7	1.0187	-0.2991	26	1.0495	-
8	1.0292	-	27	1.0481	-
9	1.0267	-	28	1.0437	-
10	1.0248	-	29	1.0200	-0.2272
11	1.0243	-	30	1.0140	-0.2515
12	0.9932	-0.6247	31	1.0023	-0.5082
13	0.9922	-0.6673	32	1.0000	-0.5750
14	0.9923	-0.6654	33	0.9982	-0.6381
15	0.9945	-0.6313			
16	1.0369	-	Other Unknowns		
17	1.0389	-	$M_{12-11} = 0.9700$		
18	1.0393	-	$M_{15-16} = 0.9600$		
19	1.0450	-0.0593	$M_{33-18} = 0.9599$		

M_{12-11} is expected to be 0.97 and found as 0.9700, M_{15-16} and M_{33-18} are expected to be 0.96 and found as 0.9600 and 0.9599 respectively. Regarding to bus voltages, most of calculated bus voltage magnitudes are the same as in the previous case where all VSCs have constant modulation indexes. Maximum voltage magnitude difference between two analyses is 0.0001 p.u. only.

4.3 Test System III

This system is the same as the Test System I except that a buck converter is connected to bus 6 on the line between bus 5 and bus 6 as shown in Figure 37. All system variables are the same as in the Test System I and all VSC converters are operating in constant modulation index mode.

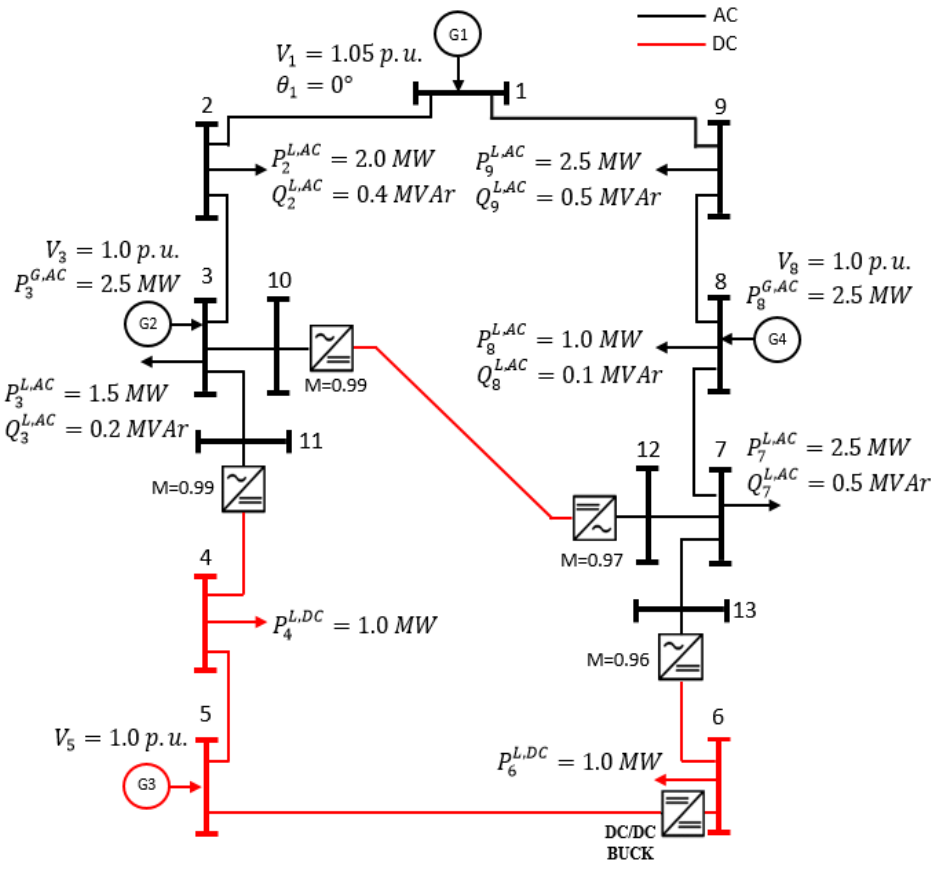

Figure 37. Representation of Test System III

The efficiency of all converters are 98%. Buck converter is also operating in constant duty ratio mode with $D_{6-5} = 0.95$. A load flow analysis is conducted on this test system using the proposed algorithm and generated active and reactive powers, voltage magnitudes and phases, line flows are given in Table 21 and Table 22.

Table 21. Generated Power and Voltage Results for Test System III

Bus	Generator	P (MW)	Q (MVAr)	Limits
1	G1	5.8818	0.7824	
3	G2	2.5000	0.9756	Qlimits=0.10-1.00
5	G3	1.0861		Plimits=0.50-2.00
8	G4	2.5000	0.9989	Qlimits=0.10-1.00

Bus	Voltage (p.u.)	Phase θ (degrees)	Bus	Voltage (p.u.)	Phase θ (degrees)
1	1.050	0.000	8	1.000	-5.307
2	1.012	-2.735	9	1.004	-3.409
3	1.000	-5.876	10	0.980	-8.533
4	0.948	-	11	0.992	-7.023
5	1.000	-	12	0.941	-7.030
6	**0.948**	-	13	0.914	-11.253
7	0.924	-9.850			

Table 22. Power Flows of Test System III

Sending	Receiving	Active Power P (MW)	Reactive Power Q (MVAr)	Sending	Receiving	Active Power P (MW)	Reactive Power Q (MVAr)
1	2	2.6351	0.3577	7	12	-0.9992	-0.2748
1	9	3.2467	0.4247	7	13	0.4861	0.1731
2	1	-2.5529	-0.2232	8	7	2.1102	0.6002
2	3	0.5529	-0.1768	8	9	-0.6102	0.2986
3	2	-0.5360	0.2044	9	1	-3.1221	-0.2207
3	10	1.0697	0.4074	9	8	0.6221	-0.2793
3	11	0.4663	0.1637	10	3	-1.0659	-0.3503
4	5	-0.5457	-	10	12	1.0659	0.3503
4	11	-0.4543	-	11	3	-0.4656	-0.1530
5	4	0.5471	-	11	4	0.4656	0.1530
5	6	0.5390	-	12	7	1.0029	0.3296
6	5	-0.5269	-	12	10	-1.0029	-0.3296
6	13	-0.4731	0.0000	13	6	0.4852	0.1595
7	8	-1.9869	-0.3983	13	7	-0.4852	-0.1595

As the power flow analysis results indicate, when DC/DC buck converter is connected to bus 6, voltage magnitude is reduced to 0.948 p.u. from where it was 0.994 p.u. for the Test System I, which does not have a buck converter connected. This result is expected since bus 5 has "1.0 p.u." voltage magnitude and duty ratio of the DC/DC buck converter is adjusted to 0.95 and there is some amount of voltage drop on the DC line. Algorithm has converged to this solution with a maximum absolute value of mismatch which is less than 10^{-10} after four iterations with a time average of 10 executions is 28.3 ms.

4.4 Test System IV

This system is a modified version of Test System II with two DC/DC converters as shown in Figure 38. Suppose that there is a need for a higher DC voltage on bus 9 and power will be transferred over a long distance to bus 10. Then, DC voltage is boosted by using a DC/DC boost converter. Afterwards, it is reduced back to a level that it is going to be utilized by a DC/DC buck converter. Reactive power limits and active power ratings of generators are given in Table 23.

Table 23. Generator Ratings of Test System IV

Generator	P (MW)	Qmax (MVAr)	Qmin (MVAr)
G2	0.5	0.5	0.01
G3	0.25	-	-
G4	0.25	-	-
G5	0.25	-	-
G6	0.5	0.5	0.01
G7	0.5	0.5	0.01

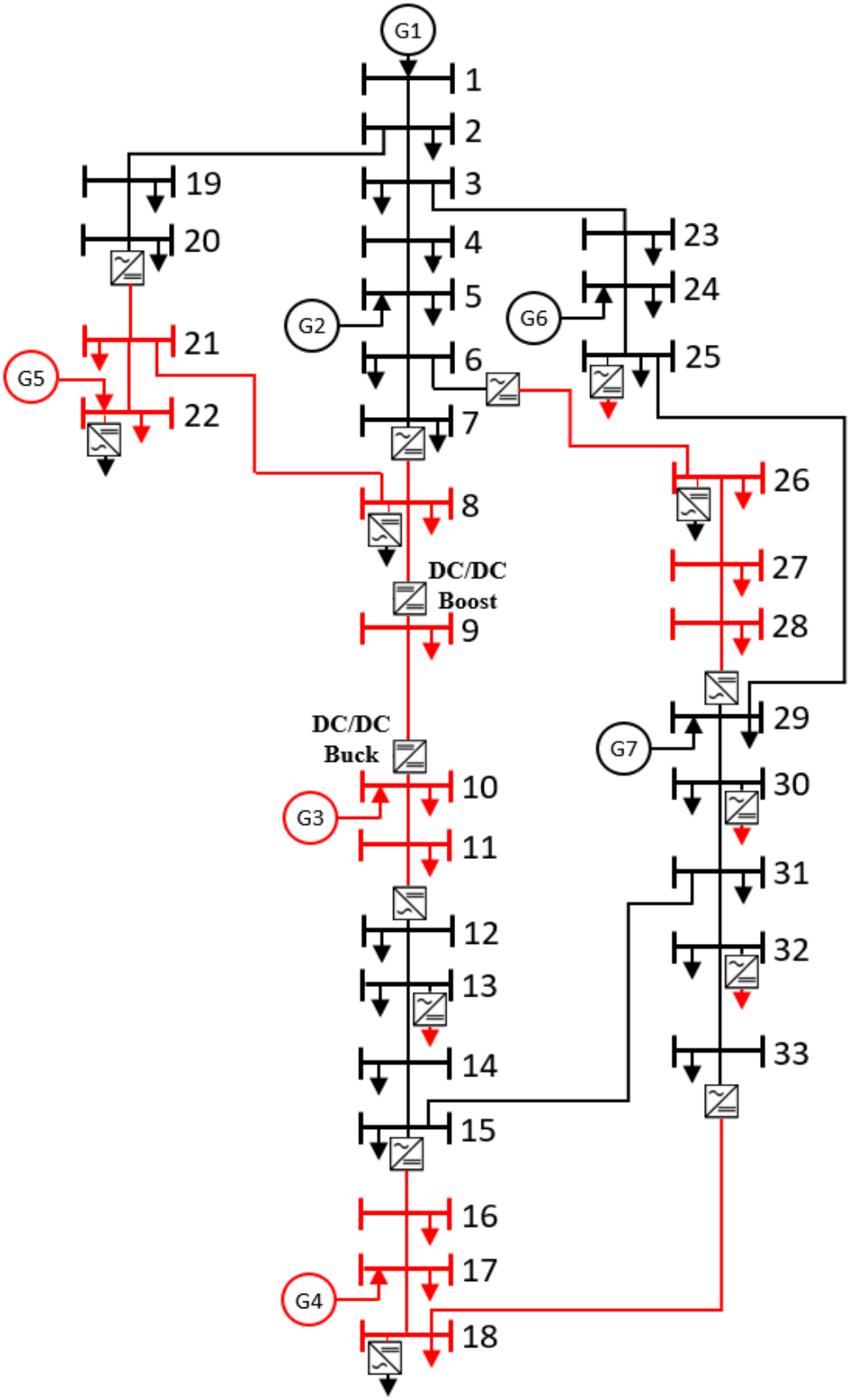

Figure 38. Representation of Test System IV

The efficiency (η) of all converters in the system are 95% and the power factor is 95% for VSCs. Modulation indexes or duty ratios of converters are given in Table 24. First bus is chosen as a reference bus and it has "1.05 p.u." voltage magnitude and "0 degrees" phase angle. Other PV buses voltage magnitudes are $V_5 = 1.03\ p.u.$, $V_{24} = 1.03\ p.u.$, $V_{29} = 1.02\ p.u.$ and line impedances and load data are the same as in the Test System II.

Load flow algorithm is converged with a maximum absolute value of mismatch which is less than 10^{-10} after six iterations. A series of 10 executions are performed and the average analysis time is found to be 56 ms. The total system loss is calculated as 0.400 MW + 0.567 MVAr. Bus voltages and phase angles calculated by using the proposed load flow analysis method are presented in Table 25 . Note that the voltage magnitude of bus 9 is increased and it reduces back at bus 10. Generated active and reactive powers are provided in Table 26 and line power flows are given in Table 27.

Table 24. Converter Modulation Indexes/Duty Ratios of Test System IV

Converter @ Bus	Converter Type	M or D
6	VSC	0.97
7	VSC	0.99
9	DC/DC BOOST	0.10
10	DC/DC BUCK	0.90
12	VSC	0.97
15	VSC	0.96
20	VSC	0.99
29	VSC	0.98
33	VSC	0.96

Table 25. Load Flow Analysis Results of Test System IV

Bus	Voltage (p.u.)	Phase θ (degrees)	Bus	Voltage (p.u.)	Phase θ (degrees)
1	1.0500	0.0000	18	1.0392	0.0000
2	1.0471	-0.0125	19	1.0450	-0.0624
3	1.0378	-0.0451	20	1.0285	-0.4459
4	1.0336	-0.0606	21	1.0368	0.0000
5	1.0300	-0.0818	22	1.0370	0.0000
6	1.0190	-0.3104	23	1.0348	-0.0766
7	1.0185	-0.3384	24	1.0300	-0.1542
8	**1.0289**	0.0000	25	1.0224	-0.2652
9	**1.1402**	0.0000	26	1.0494	0.0000
10	**1.0246**	0.0000	27	1.0480	0.0000
11	1.0241	0.0000	28	1.0437	0.0000
12	0.9930	-0.6817	29	1.0200	-0.2782
13	0.9920	-0.7234	30	1.0140	-0.3027
14	0.9921	-0.7207	31	1.0022	-0.5606
15	0.9944	-0.6861	32	1.0000	-0.6275
16	1.0368	0.0000	33	0.9981	-0.6908
17	1.0387	0.0000			

Table 26. Generation Data for Test System IV

Bus	Generator	P (MW)	Q (MVAr)	Limits
1	G1	4.3929	1.8237	-
5	G2	0.5000	0.1901	Qlimits=0.01-0.50
10	G3	0.2500	-	-
17	G4	0.2500	-	-
22	G5	0.2500	-	-
24	G6	0.5000	0.2491	Qlimits=0.01-0.50
29	G7	0.5000	0.1094	Qlimits=0.01-0.50

Table 27. Power Flows of Test System II

Sending	Receiving	Active Power P (MW)	Reactive Power Q (MVAr)	Sending	Receiving	Active Power P (MW)	Reactive Power Q (MVAr)
1	2	4.3929	1.8237	17	16	0.3333	0.0000
2	1	-4.3811	-1.8177	17	18	-0.1433	0.0000
2	3	2.6041	1.1253	18	17	0.1433	0.0000
2	19	1.5770	0.5724	18	33	-0.2357	0.0000
3	2	-2.5815	-1.1138	19	2	-1.5744	-0.5699
3	4	1.5524	0.6632	19	20	1.3944	0.4899
3	23	0.8492	0.3705	20	19	-1.3756	-0.4730
4	3	-1.5463	-0.6602	20	21	1.1956	0.3930
4	5	1.3063	0.5002	21	8	0.8765	0.0000
5	4	-1.3020	-0.4979	21	20	-1.1335	0.0000
5	6	1.6770	0.6281	21	22	-0.0430	0.0000
6	5	-1.6615	-0.6148	22	16	0.0223	0.0000
6	7	0.1575	0.0861	22	21	0.0430	0.0000
6	26	1.3040	0.4286	23	3	-0.8469	-0.3690
7	6	-0.1575	-0.0860	23	24	0.6669	0.2690
7	8	-0.0425	-0.0140	24	23	-0.6642	-0.2669
8	7	0.0448	0.0000	24	25	1.0492	0.4559
8	9	0.5788	0.0000	25	24	-1.0423	-0.4505
8	21	-0.8698	0.0000	25	29	0.4265	0.3505
9	8	-0.5484	0.0000	26	6	-1.2375	0.0000
9	10	0.4284	0.0000	26	27	1.1143	0.0000
10	9	-0.4063	0.0000	27	26	-1.1128	0.0000
10	11	0.5363	0.0000	27	28	0.9128	0.0000
11	10	-0.5360	0.0000	28	27	-0.9091	0.0000
11	12	0.2360	0.0000	28	29	0.7891	0.0000
12	11	-0.2242	-0.0737	29	25	-0.4256	-0.3496
12	13	0.1042	0.0037	29	28	-0.7476	-0.2457
13	12	-0.1041	-0.0036	29	30	1.5882	0.6698
13	14	-0.0191	-0.0114	30	29	-1.5791	-0.6652
14	13	0.0191	0.0114	30	31	1.3739	0.6052
14	15	-0.4191	-0.2114	31	15	0.4027	0.2278
15	14	0.4199	0.2121	31	30	-1.3606	-0.5920
15	16	-0.2799	-0.0920	31	32	0.7879	0.3142
15	31	-0.4000	-0.2251	32	31	-0.7865	-0.3126
16	15	0.2949	0.0000	32	33	0.4889	0.2426
16	17	-0.3326	0.0000	33	18	0.2482	0.0816
16	22	-0.0223	0.0000	33	32	-0.4882	-0.2416

4.5 Discussion of Analysis Results

All in all, the method presented here is implemented in four different test systems. First test system has thirteen buses, which are supplied by three AC and one DC generators. Four VSCs are utilized in the test system for AC/DC conversion and they are operating in constant modulation index mode. Proposed algorithm results are compared to two other approaches and results show consistency with each other. Then, operating modes of two converters are changed to maintain constant voltage magnitudes at their output terminals and converter modulation indexes are successfully calculated with the proposed algorithm. Afterwards, it is applied for a 33-bus test system and again the algorithm provides consistent results with the reduced gradient approach. The presented Newton-Raphson based methodology has the advantage of quadratic convergence therefore; it produces results faster than the other approach only in a few iterations. Finally, different DC/DC converters are connected on these two test systems and the presented load flow analysis method is again applied. All bus voltage magnitudes, phase angles, AC and DC line power flows and generation data are calculated successfully.

CHAPTER 5

CONCLUSION

As the electric power system utilizes more and more renewable and distributed energy sources, new challenges arise on the present AC distribution system. Solar power plants, battery storage systems, plenty of modern electronic devices in homes or offices and electric fast charging stations utilize DC power and their integration requires additional power conversion stages. Besides, electrical distribution system is evolved from a unidirectional structure to a bidirectional one. For instance, an electric charging station may demand power from the utility when electric vehicles connected are getting charged or may support the utility when excess energy is available on electric vehicle batteries. Battery storage systems are also demanding bidirectional power flow since they have charging and discharging processes. Increasing utilization of these systems indicated the requirement of upgrading current AC oriented electric distribution system into a more smart and hybrid structure.

AC/DC distribution systems are complex structures, which have various power electronic devices, AC or DC generators, loads, different type of AC or DC buses and lines. Therefore, load flow analysis is required to be able to obtain necessary information about the steady state conditions of an electrical power network. Future smart distribution systems will require real time assessment of the network; hence, a load flow analysis method should produce fast but accurate results to be able to sustain secure and reliable power system operations.

This thesis presented a load flow analysis approach based on Newton-Raphson iterative method with combined AC/DC power flow equations for AC/DC distribution systems. For this purpose, different AC and DC bus classifications are introduced. VSCs and DC/DC converters are presented with their respective models and implemented in various test systems. Application of the Newton-Raphson based load flow approach to an AC/DC hybrid distribution system is explained and a modified Jacobian matrix is introduced. AC and DC power flow equations for different connection scenarios are presented and their derivatives with respect to possible system unknowns are obtained for various system configurations.

The load flow technique presented here can be applied to radial or meshed network configurations and it is able to obtain voltage magnitudes and phase angles of AC buses, DC bus voltages, AC and DC line power flows and losses. Proposed approach has been implemented in four sample distribution systems with AC/DC and DC/DC converters operating at different modes and it has successfully calculated AC and DC bus voltages, generation data and line power flows. It is able to calculate necessary modulation index and duty ratio values of converters for constant output voltage mode operations and it takes into account converter losses as well. Results of the presented algorithm have been compared to and verified against the solutions of the generalized reduced gradient method and PSCAD software. Algorithm solution is consistent with these approaches and it produces results faster, which is a valuable feature for load flow analysis.

Future smart grids are expected to become more complex and technology driven, therefore the way they are interpreted and analysed will change as well. For future studies, different generator and load models that will be utilized in smart AC/DC grids can be implemented. AC and DC power flow equations can be extended so that any other converter model can be implemented with this method. The approach presented here may help to determine steady state operating conditions of future smart AC/DC grids and to maintain these power networks in reliable conditions.

REFERENCES

[1] H. M. A. Ahmed, A. B. Eltantawy and M. M. A. Salama, "A Generalized Approach to the Load Flow Analysis of AC–DC Hybrid Distribution Systems," *IEEE Transactions on Power Systems,* vol. 33, no. 2, pp. 2117-2127, 2018.

[2] M. Baradar and M. Ghandhari, "A Multi-Option Unified Power Flow Approach for Hybrid AC/DC Grids Incorporating Multi-Terminal VSC-HVDC," *IEEE Transactions on Power Systems,* vol. 28, no. 3, pp. 2376-2383, 2013.

[3] M. Baradar, M. Ghandhari and D. V. Hertem, "The Modeling Multi-terminal VSC-HVDC in Power Flow Calculation Using Unified Methodology," in *2011 2nd IEEE PES International Conference and Exhibition on Innovative Smart Grid Technologies,* Manchester, 2011.

[4] C. Sulzberger, "Triumph of AC - from Pearl Street to Niagara," *IEEE Power and Energy Magazine,* vol. 1, no. 3, pp. 64-67, 2003.

[5] Brainkart, "AC and DC Distribution," [Online]. Available: https://www.brainkart.com/article/AC-and-DC-Distribution_12344/. [Accessed 2 January 2019].

[6] International Renewable Energy Agency (IRENA), "Electricity Storage and Renewables: Costs and Markets to 2030," October 2017. [Online]. Available: https://www.irena.org/publications/2017/Oct/Electricity-storage-and-renewables-costs-and-markets. [Accessed 6 January 2019].

[7] SolarPower Europe, "Global Market Outlook For Solar Power 2018-2022," 27 June 2018. [Online]. Available: http://www.solarpowereurope.org/global-market-outlook-2018-2022/. [Accessed 3 February 2019].

[8] P. Wang, L. Goel, X. Liu and F. H. Choo, “Harmonizing AC and DC: A Hybrid AC/DC Future Grid Solution,” *IEEE Power and Energy Magazine,* vol. 11, no. 3, pp. 76-83, 2013.

[9] L. O. Barthold, D. A. Woodford and M. Salimi, “DC Is Where We Started: Is It Also Where We're Going?,” *IEEE Power and Energy Magazine,* vol. 14, no. 2, pp. 110-112, 2016.

[10] V. A. Prabhala, B. P. Baddipadiga, P. Fajri and M. Ferdowsi, “An Overview of Direct Current Distribution System Architectures & Benefits,” *Energies,* vol. 11, no. 9, 2018.

[11] D. Salomonsson and A. Sannino, “Load Modelling for Steady-state and Transient Analysis of Low-voltage DC Systems,” *IET Electric Power Applications* , vol. 1, no. 5, pp. 690-696, 2007.

[12] D. J. Hammerstrom, “AC Versus DC Distribution Systems Did We Get it Right?,” in *2007 IEEE Power Engineering Society General Meeting,* Tampa, FL, USA, 2007.

[13] M. Starke, L. M. Tolbert and B. Ozpineci, “AC vs. DC distribution: A loss Comparison,” in *2008 IEEE/PES Transmission and Distribution Conference and Exposition*, Chicago, IL, USA, 2008.

[14] K. Daware , “DC Power Distribution Systems,” [Online]. Available: https://www.electricaleasy.com/2018/02/dc-power-distribution-systems.html. [Accessed 2 March 2019].

[15] G. F. Reed, B. M. Grainger, A. R. Sparacino and Z.-H. Mao, “Ship to Grid: Medium-Voltage DC Concepts in Theory and Practice,” *IEEE Power and Energy Magazine,* vol. 10, no. 6, pp. 70-79, 2012.

[16] European Commision, “Low Voltage Directive 73/23/EEC,” 19 February 1973. [Online]. Available: https://www.ab.gov.tr/files/tarama/tarama_files/01/SC01EXP_LVD.pdf. [Accessed 4 April 2019].

[17] T. Kaipia, P. Salonen, J. Lassila and J. Partanen, “Possibilities of the Low Voltage DC Distribution Systems,” in *NORDAC 2006*, Stockholm, 2006.

[18] T. Kaipia, P. Salonen, J. Lassila and J. Partanen, “Application of Low Voltage DC-Distribution system–A Techno-economical Study,” in *19th International Conference on Electricity Distribution*, Vienna, 2007.

[19] IEEE European Public Policy Initiative, “DC Electricity Distribution in the European Union,” 27 March 2017. [Online]. Available: https://www.ieee.org/content/dam/ieee-org/ieee/web/org/about/eppi_dc_electricitiy_distribution_june_2017.pdf. [Accessed 15 March 2019].

[20] S. K. Chaudhary, J. M. Guerrero and R. Teodorescu, “Enhancing the Capacity of the AC Distribution System Using DC Interlinks—A Step Toward Future DC Grid,” *IEEE Transactions on Smart Grid*, vol. 6, no. 4, pp. 1722-1729, 2015.

[21] T. F. Garrity, “Getting Smart,” *IEEE Power and Energy Magazine*, vol. 6, no. 2, pp. 38-45, 2008.

[22] H. Farhangi, “The Path of the Smart Grid,” *IEEE Power and Energy Magazine*, vol. 8, no. 1, pp. 18-28, 2010.

[23] A. Bracale, P. Caramiaa, G. Carpinelli, F. Mottola and D. Proto, “A Hybrid AC/DC Smart Grid to Improve Power Quality and Reliability,” in *2012 IEEE International Energy Conference and Exhibition (ENERGYCON)*, Florence, 2012.

[24] T. Adefarati and R. Bansal, “Integration of Renewable Distributed Generators into the Distribution System: A Review,” *IET Renewable Power Generation,* vol. 10, no. 7, pp. 873-884, 2016.

[25] A. Sannino, G. Postiglione and M. Bollen, “Feasibility of a DC Network for Commercial Facilities,” *IEEE Transactions on Industry Applications,* vol. 39, no. 5, pp. 1499-1507, 2003.

[26] M. A. Rodriguez-Otero and E. O'Neill-Carrillo, “Efficient Home Appliances for a Future DC Residence,” in *2008 IEEE Energy 2030 Conference*, Atlanta, 2008.

[27] D. Salomonsson and A. Sannino, “Low-Voltage DC Distribution System for Commercial Power Systems With Sensitive Electronic Loads,” *IEEE Transactions on Power Delivery,* vol. 22, no. 3, pp. 1620-1627, 2007.

[28] T. Taufik and M. Muscarella, “Development of DC House Prototypes as Demonstration Sites for an Alternate Solution to Rural Electrification,” in *2016 6th International Annual Engineering Seminar (InAES)*, Yogyakarta, 2016.

[29] S. Kaur, T. Kaur, R. Khanna and P. Singh, “A State of the Art of DC Microgrids for Electric Vehicle Charging,” in *2017 4th International Conference on Signal Processing, Computing and Control (ISPCC),* Solan, 2017.

[30] L. Qi, A. Antoniazzi and L. Raciti, “DC Distribution Fault Analysis, Protection Solutions, and Example Implementations,” *IEEE Transactions on Industry Applications,* vol. 54, no. 4, pp. 3179-3186, 2018.

[31] D. Kumar, F. Zare and A. Ghosh, “DC Microgrid Technology: System Architectures, AC Grid Interfaces, Grounding Schemes, Power Quality, Communication Networks, Applications, and Standardizations Aspects,” *IEEE Access,* vol. 5, pp. 12230-12256, 2017.

[32] G. Raman, G. Raman, J. C.-H. Peng and W. Xiao, “Bridging the Transition to DC Distribution: A Hybrid Microgrid for Residential Apartments,” in *2017 IEEE Innovative Smart Grid Technologies - Asia (ISGT-Asia)*, Auckland, 2017.

[33] A. Ghadiri, M. R. Haghifam and S. M. M. Larimi, “Comprehensive Approach for Hybrid AC/DC Distribution Network Planning Using Genetic Algorithm,” *IET Generation, Transmission & Distribution,* vol. 11, no. 6, pp. 3892-3902, 2017.

[34] K. Kurohane, T. Senjyu, A. Yona, N. Urasaki, T. Goya and T. Funabashi, “A Hybrid Smart AC/DC Power System,” *IEEE Transactions on Smart Grid,* vol. 1, no. 2, pp. 199-204, 2010.

[35] O. Khan, S. Z. Jamali and C.-H. Noh, “A Load Flow Analysis for AC/DC Hybrid Distribution Network Incorporated with Distributed Energy Resources for Different Grid Scenarios,” *Energies,* vol. 11, no. 2, 2018.

[36] J. Beerten, D. V. Hertem and R. Belmans, “VSC MTDC Systems with a Distributed DC voltage Control - A Power Flow Approach,” in *2011 IEEE Trondheim PowerTech*, Trondheim, 2011.

[37] C. Liu, B. Zhang, Y. Hou, F. F. Wu and Y. Liu, “An Improved Approach for AC-DC Power Flow Calculation With Multi-Infeed DC Systems,” *IEEE Transactions on Power Systems ,* vol. 26, no. 2, pp. 862-869, 2011.

[38] J. Beerten, S. Cole and R. Belmans, “Generalized Steady-state VSC MTDC Model for Sequential AC/DC Power Flow Algorithms,” *IEEE Transactions on Power Systems,* vol. 27, no. 2, pp. 821-829, 2012.

[39] L. Gengyin, Z. Ming, H. Jie, L. Guangkai and L. Haifeng, “Power Flow Calculation of Power Systems Incorporating VSC-HVDC,” in *2004 International Conference on Power System Technology, 2004,* Singapore, 2004.

[40] K. N. Narayanan and P. Mitra, “A Comparative Study of a Sequential and Simultaneous AC-DC Power Flow Algorithms for a Multi-terminal VSC-HVDC System,” in *2013 IEEE Innovative Smart Grid Technologies-Asia (ISGT Asia)*, Bangalore, 2013.

[41] S. Bahrami, V. W. S. Wong and J. Jatskevich, “Optimal Power Flow for AC-DC Networks,” in *2014 IEEE International Conference on Smart Grid Communications (SmartGridComm)*, Venice, 2014.

[42] A. R. Bergen and V. Vittal , Power Systems Analysis, 2nd ed., New Jersey: Pearson, 1999.

[43] N. Mohan, T. M. Undeland and W. P. Robbins, Power Electronics Converters, Applications, and Design, 3rd ed., Hoboken, NJ: John Wiley & Sons, 2003.

[44] D. G. Holmes and T. A. Lipo, Pulse Width Modulation for Power Converters: Principles and Practice, vol. 18, New York, NY: John Wiley & Sons, 2003.